Published in final edited form as:
Eur J Neurosci. 2013 January ; 37(1): 80–95. doi:10.1111/ejn.12024.

Effects of the α_2-adrenergic receptor agonist dexmedetomidine on neurovascular responses in somatosensory cortex

Mitsuhiro Fukuda, Ph.D.[1], **Alberto L. Vazquez, Ph.D.**[1], **Xiaopeng Zong, Ph.D.**[1], and **Seong-Gi Kim, Ph.D.**[1,2]

[1]Neuroimaging Laboratory, Department of Radiology, University of Pittsburgh, Pittsburgh PA USA 15213

[2]Neuroimaging Laboratory, Department of Neurobiology, University of Pittsburgh, Pittsburgh PA USA 15213

Abstract

This paper describes the effects of dexmedetomidine (DEX) 5 the active ingredient of medetomidine which is the latest popular sedative for functional magnetic resonance imaging (fMRI) in rodents 5 on multiple unit activity, local field potential (LFP), cerebral blood flow (CBF), pial vessel diameter (indicative of cerebral blood volume; CBV), and blood-oxygenation-level-dependent (BOLD) fMRI. These measurements were obtained from the rat somatosensory cortex during 10-s forepaw stimulation. We found that the continuous intravascular systemic infusion of DEX (50μg/kg/h, doses typically used in fMRI studies) caused epileptic activities and that supplemental isoflurane administration of ~0.3% helped suppress the development of epileptic activities and maintained robust neuronal and hemodynamic responses up to 3 hours. Supplemental administration of nitrous oxide (N_2O) in addition to DEX nearly abolished hemodynamic responses even if neuronal activity remained. Under DEX-ISO anesthesia, spike firing rate and the delta power of LFP increased, while beta and gamma power decreased compared to ISO-only anesthesia. DEX administration caused pial arteries and veins to constrict nearly equally, resulting in decreases in baseline CBF and CBV. Evoked LFP and CBF responses to forepaw stimulation were largest at a frequency of 8–10 Hz, and a non-linear relationship was observed. Similarly, BOLD fMRI responses measured at 9.4 Tesla were largest at a frequency of 10 Hz. Both pial arteries and veins dilated rapidly (artery, 32.2%; vein, 5.8%), while venous diameter changes returned to baseline slower than arteries. These results will be useful for designing, conducting and interpreting fMRI experiments under DEX sedation.

Keywords

Rat; medetomidine; BOLD; functional connectivity; CBV

INTRODUCTION

Anesthesia is commonly used in functional brain imaging studies that investigate a wide variety of neuroscience research questions including neuro-vascular relationships, pain mechanisms, consciousness, longitudinal functional development and re-organization. Imaging studies are often performed in immobilized animals to avoid motion artifacts. Since immobilization without stress is not often possible particularly for relatively long recording sessions in alert animals, the use of anesthesia is beneficial. Anesthesia, however, can

Corresponding Author: Mitsuhiro Fukuda, Ph.D., 3025 E Carson St, McGowan Institute Room 155, Pittsburgh, PA 15203, Pone: 412-383-6695, Fax: 412-383-6799, mif5@pitt.edu.

modify neuronal and hemodynamic activity (Berwick *et al.*, 2002; Martin *et al.*, 2006). Thus, it is critical to understand the impact of anesthesia on neuronal and hemodynamic responses.

Two anesthetic agents, isoflurane (ISO) and medetomidine hydrochrolide (MED) are often used for functional magnetic resonance imaging (fMRI) experiments because of their ability to perform longitudinal studies. Our group previously explored the impact of ISO anesthesia on neuro-vascular responses in the rat forepaw model (Masamoto *et al.*, 2007; Masamoto *et al.*, 2009; Kim *et al.*, 2010). ISO around 1 minimum alveolar concentration (1.38%, White *et al.*, 1974) provides a stable physiological condition for experiments >6 hours. However, ISO strongly suppresses neuronal activity (Banoub *et al.*, 2003) and dilates blood vessels (Iida *et al.*, 1998) which reduce evoked hemodynamic responses. Thus, the ISO use for fMRI studies has been limited. Meanwhile, MED has recently become popular for rodent fMRI studies over various brain regions, including brain stem, hippocampus, basal ganglia, and neocortex (Van Camp *et al.*, 2006; Weber *et al.*, 2006; Zhao *et al.*, 2008; Angenstein *et al.*, 2010) largely because MED yields robust hemodynamic responses; however, this effect only lasts for <3 hours (Pawela *et al.*, 2009). Despite the popular use of MED, its effects on physiological parameters, such as cerebral blood flow (CBF), cerebral blood volume (CBV) and neuronal activity under doses typically used in fMRI studies (100 μg/kg/h) have not been established.

The pharmacological effects of MED are attributed to its optical isomer, dexmedetomidine hydrochrolide (DEX), and thus both MED and DEX exert the same physiological effects (Vickery & Maze, 1989; MacDonald *et al.*, 1991; Savola & Virtanen, 1991; Schmeling *et al.*, 1991). DEX is a highly selective α_2-adrenergic receptor agonist that crosses the blood-brain barrier. DEX produces sedation and analgesia dose-dependently with a minimal effect on the respiratory system despite its muscular relaxation (Doze *et al.*, 1989; Kalso *et al.*, 1991; Correa-Sales *et al.*, 1992; Guo *et al.*, 1996). For this reason, DEX has been used in veterinary and clinical settings as an anesthetic adjuvant (Sinclair, 2003; Bekker & Sturaitis, 2005). In neuroimaging studies, DEX can be used as a supplement for reducing volatile anesthetics (Segal *et al.*, 1988; Savola *et al.*, 1991) and this combination may also prolong the desired effects of DEX. Thus, DEX-ISO anesthesia is attractive for fMRI studies, but its impact on neuronal activity and hemodynamic responses is not known. In the present study, we investigated the effects of DEX under doses relevant to published fMRI studies on baseline and evoked neuro-vascular activities by obtaining neuronal, CBF, vessel diameter and fMRI measurements from the rat somatosensory cortex.

METHODS

Twenty five male Sprague-Dawley rats (260–450 g, Charles River Laboratories, Wilmington, MA) were used following an animal protocol approved by the University of Pittsburgh Institutional Animal Care and Use Committee in accordance with the National Institutes of Health Guide for the Care and Use of Laboratory Animals. Twenty-one rats were used for non-fMRI studies, while four rats were used for fMRI studies with DEX-ISO anesthesia.

Animal preparation

The rats were initially anesthetized using 5% ISO in oxygen-enriched air (30–35% inspired oxygen (O_2)) for intubation. Then, lidocaine gel (2%) was applied locally for placement of catheters in a femoral artery and vein under 2–2.5% ISO. Atropine was not used in the present studies because its anticholinergic effect can cause adverse cardiovascular effects with DEX administration (for a review, see Sinclair, 2003). The respiration rate and ventilation volume of the ventilator (TOPO, Kent Scientific, Torrington, CT) were adjusted to maintain normal blood gas levels throughout experiments. Approximately 0.1 ml of blood

was withdrawn from the femoral artery to measure the systemic arterial blood oxygen tension (P_{aO2}), arterial carbon dioxide tension (P_{aCO2}) and pH using a blood gas analyzer (Stat Profile, Nova Medical Corp., Waltham, MA). For non-fMRI physiological studies, the rats were placed in a stereotaxic frame (SR-5R, Narishige, Tokyo, Japan). Lidocaine gel (2%) was applied at pressure points of the stereotaxic frame and 0.3 ml of 2% lidocaine was administered under the skin over the targeted craniotomy location. A custom-made recording chamber (2.2 cm outer diameter) was mounted on the exposed skull over the forepaw cortical area using dental acrylic. A 5 mm × 7 mm portion of the skull, centered 3.5-mm lateral and 1.5-mm rostral from bregma, was thinned with a dental drill and then removed using forceps. The cerebrospinal fluid was released by performing a dural puncture of the cisterna magna prior to duratomy to minimize herniation. The dura mater over the forepaw cortical area was resected. The chamber as well as the dural puncture site were then sealed with agarose gel (typically 0.4%) at body temperature.

The anesthesia and breathing gas mixture were adjusted to 1.3 – 1.4% ISO in oxygen-enriched air (25–30% inspired O_2) for at least 30 min before starting experiments. During experimental recordings, the mean arterial blood pressure (MABP), heart rate, respiration rate, end-tidal carbon dioxide (CO_2), O_2, nitrous oxide (N_2O) and ISO levels were monitored (Capnomac Ultima, Datex Engstrom, Inc. Tewksbury, MA) and recorded using a polygraph data acquisition system (MP150 and ACK100W Acknowledge, Biopac Systems Inc., Goleta, CA). Rectal temperature was maintained at 37.0 °C using a feedback-controlled heating pad (40-90-8C, FHC, Inc., Bowdoinham, ME).

Experimental recordings of evoked somato-sensory activity were performed under ISO at 1.3 – 1.4%. After these experiments, DEX at 50 μg/kg (DEXDOMITOR® (dexmedetomidine), Pfizer Inc., NY) was injected intravenously (IV) as a bolus, and the ISO level was reduced to 0.5%. Fifteen minutes after the bolus injection, continuous infusion of DEX at a rate of 50 μg/kg/h (IV) commenced. The infusion liquid also contained pancuronium bromide (1.5 mg/kg/h) and 5% of dextrose. It should be noted that a dose rate of 50μg/kg/h DEX is equivalent to 100 μg/kg/h MED, which is the typical dose rate used in most published fMRI studies (Ramos-Cabrer *et al.*, 2005; Weber *et al.*, 2006; Pawela *et al.*, 2008; Weber *et al.*, 2008; Zhao *et al.*, 2008; Pawela *et al.*, 2009; Airaksinen *et al.*, 2010; Angenstein *et al.*, 2010; Seehafer *et al.*, 2010; Williams *et al.*, 2010; Krautwald & Angenstein, 2011; Nasrallah *et al.*, 2012).

For electric stimulation, two needle electrodes were inserted between digits 2 and 4 under the palmar skin of either the left or right forepaw for electrical stimulation. Electrical pulses were generated using a waveform generator (Master 8, A.M.P.I., Israel) and delivered using a constant current isolator (Iso-Flex, A.M.P.I., Israel) to the forepaw contralateral to the recording site. Electric pulses with width of 1 ms and current of ≤1.5 mA were delivered for 10 seconds. No MABP change due to the stimulation was observed.

Experimental designs

Three major experiments were performed; i) evoked neural activity and hemodynamic responses were recorded under DEX only vs. DEX + ISO vs. DEX + N_2O, ii) spontaneous neural activity and baseline hemodynamics were recorded under ISO only vs. DEX + ISO, and iii) evoked neural activity and hemodynamic responses under DEX + ISO were characterized. All functional studies under DEX were performed at least 30 min after the bolus injection of DEX. Neural activities (i.e. local field potentials (LFP) and multiple-unit activity (MUA)) were measured using a metal microelectrode; CBF was measured by laser Doppler flowmetry (LDF); vessel diameters were measured using optical imaging; and blood oxygenation level dependent (BOLD) fMRI was measured using a 9.4-T MRI scanner.

Specific experiments (for a summary, see Table 1):

Experiment #1.1: Evoked LFP and CBF responses under DEX only—To examine whether robust and stable evoked hemodynamic responses can be obtained under DEX only anesthesia, electrical stimulation at a frequency of 3, 4, 6, 8, 9, 10, or 12 Hz for 10 s with 70 s ISI was intermittently delivered to the forepaw to evoke LFP and CBF responses in the somatosensory cortex. These experiments were conducted in 5 rats and experimental recording lasted more than 120 min during which DEX alone was continuously infused (50 μg/kg/h). To attempt to extend the effects of DEX demonstrated by Pawela et al. (2009), the infusion dose rate was increased from 50 μg/kg/h to 150 μg/kg/h (equivalent to 300 μg/kg/h MED) 120–156 min after the initial DEX bolus administration in 3 rats, and cortical evoked responses to forepaw stimulation (4, 6, 8, 10, or 12 Hz for 10 s with 70 s ISI) were recorded. The stimulation frequency over all experiments was randomized between trials. At least two trials were recorded for each frequency in all experiments.

Experiment #1.2: Comparison between DEX + ISO vs. DEX + N_2O conditions—To examine the effect of inspired N_2O gas on evoked responses in DEX-sedated rats, LFP and CBF responses to forepaw stimulation at four different frequencies (3, 6, 9, or 12 Hz for 10 s with 70 s ISI) were recorded under DEX+N_2O (30% O_2 + 70% N_2O) and DEX+ISO (<0.5% ISO in 30% O_2 + 70% N_2) in 7 rats. It should be noted that ISO did not go down to zero for a long time after the anesthetic vaporizer was completely turned off (> 1 hour). Since 0.1% ISO has nearly no synergistic effect in combination with N_2O (Sloan *et al.*, 2010), experiments under DEX+N_2O were initiated when the ISO level was less than 0.1%.

Experiment #1.3: Effective duration of DEX + ISO for functional studies—To examine the stability of evoked responses over time, LFP and CBF responses to forepaw stimulation (8 Hz for 10 s with 70 s ISI) were monitored for more than 180 min during continuous infusion of DEX (50 μg/kg/h) with ISO (0.1 – 0.5%) in 6 rats. Two to five 8-Hz stimulation runs were recorded and averaged. To compare the effects of DEX + ISO vs. ISO only, LFP and CBF responses evoked by 10-s 8 Hz stimulation (ISI of 70 s) were also recorded under ISO only conditions. Five runs were averaged.

Experiment #2.1: Baseline MUA and LFP measurements before and after DEX administration—To examine effects of DEX on spontaneous neural activities, MUA and LFP were recorded for 5 min under ISO only and DEX + ISO conditions in the absence of evoked stimulation in 9 rats.

Experiment #2.2: Baseline CBF and vessel diameter measurements before and after DEX administration—To examine effects of DEX on baseline CBF and pial vessel diameters, LDF was recording simultaneously with pial vessel imaging under ISO only and DEX + ISO conditions in 15 rats. The baseline CBF level and pial vessel diameters were compared between these the two conditions.

Experiment #3.1: Frequency-dependent evoked LFP and CBF measurements under DEX + ISO—LFP and CBF responses to forepaw stimulation at five different frequencies (4, 6, 8, 10, and 12 Hz for 10 s with 70 s ISI) were recorded under DEX + ISO conditions in 7 rats.

Experiment #3.2: Frequency-dependent BOLD fMRI measurements under DEX + ISO—BOLD fMRI responses to forepaw stimulation at five different stimulation frequencies (4, 6, 8, 10, and 12 Hz for 10 s with 80 s ISI) were recorded under DEX + ISO conditions in 4 rats. A total of 20 to 46 runs were repeated for each frequency.

Experiment #3.3: Evoked arterial and venous vessel diameter measurements under DEX + ISO—Pial vessel diameters were measured during 10-s forepaw stimulation at a frequency of 8 Hz and ISI of 70 s in 11 rats. Five runs were repeated.

Data acquisitions

Optical imaging—Prior to the physiological experiments described above, the forepaw area was mapped using flavoprotein autofluorescence imaging over the primary somatosensory cortex under ISO of 1.3 – 1.4% (Vazquez *et al.*, 2010b; Vazquez *et al.*, 2012). Flavoprotein autofluorescence images were acquired using an epi-fluorescence microscope (MVX-10, Olympus, Tokyo, Japan) equipped with a 1× (0.25NA) objective (Olympus, Tokyo, Japan) and a digital cooled-CCD camera (1392 × 1040 imaging pixels, 6.45 × 6.45-μm^2/pixel, CoolSnap HQ2, Photometrics, Princeton, NJ). A mercury lamp light source coupled to a low-noise power supply (100W, Opti-quip, Highland Mills, NY) was used. The transmitted light was filtered between 450 and 490 nm while the camera recorded the fluorescence emission between 500 and 550 nm. Images were captured at 10 frames per second (fps) with a field-of-view of 5.7 × 4.3 mm^2 to 8.9 × 6.7 mm^2 depending on the microscope magnification. The camera's exposure time was set to 100 ms for an effective pixel resolution between 15.4 and 25.6 μm. Forepaw stimulation was performed at the optimal frequency of 12 Hz for 2 s with ISI of 16 s. Ten runs were repeated and averaged to improve signal-to-noise ratio (SNR).

Images of the cortical surface were captured to measure the diameter of pial vessels (Experiments #2.2 and #3.3). For this purpose, oblique light guides transmitting filtered yellow-green light (570 ± 10 nm) connected to a halogen light source (250W, Thermo-Oriel, Stratford, CT) were used for illumination. At this wavelength, light absorption of oxy and deoxy-hemoglobin are nearly equal and thus both arteries and veins are equally visible. To prevent artifacts stemming from the LDF probe (780 nm laser light), a low-pass interference filter (< 700 nm) was placed in front of the camera. Images were captured over a field-of-view of 1.7 × 1.2 mm^2 to 8.9 × 6.6 mm^2 with the effective pixel resolution between 2.56 μm and 6.40 μm for the baseline study (Experiment. #2.2), while images were acquired over a field-of-view of 1.9 × 1.6 mm^2 to 3.3 × 2.5 mm^2 at 10 fps with the effective pixel resolution of 2.6 to 5.1 μm for the functional study (Experiment. #3.3).

MUA, LFP and CBF measurements (All experiments except for #3.2)—Based on the functional map generated, a microelectrode with the tip diameter of 5 μm (Carbostar-1, Kation Scientific, Inc. Minneapolis, MN) was placed at a depth of ~0.3 mm below the cortical surface of the forepaw area (Fig. 1) to record neural activity extracellularly. Neural activity was recorded using an electrophysiological data acquisition system (MAP, Plexon, Inc., Dallas, TX) at a 1 kHz sampling rate. Baseline neural activity (Experiment #2.1) was acquired for a 5 min period. Multiple unit activity (MUA) data was band-pass filtered between 400 Hz – 1 kHz, while LFP activity was band-pass filtered between 3.3 – 88 Hz.

A needle-type LDF probe with tip diameter of 450 μm (PeriFlux 4001 Master system, Perimed, Sweden) was placed on the cortical surface over the forepaw area avoiding large pial vessels to measure parenchymal CBF (Fig. 1). Relative changes in CBF were acquired by the LDF system with a time constant of 0.03 s and recorded using the polygraph data acquisition software at a frequency of 100 Hz.

BOLD fMRI (Experiment #3.2)—BOLD fMRI experiments were performed on a 9.4 Tesla MRI system with a Unity INOVA console (Varian, Palo Alto, CA, USA). The gradient coil used is actively shielded with an inner diameter of 12 cm, a maximum gradient strength of 40 Gauss/cm, and a rise time of 0.12 ms (Magnex, Abington, UK). A surface coil

(2.3-cm diameter) was positioned on top of the rat's head for imaging. The magnetic field homogeneity was optimized by localized shimming to yield a typical water spectrum line-width of about 20 Hz. All fMRI images were acquired with a gradient echo echo-planar imaging (EPI) sequence with an echo time of 20 ms, a repetition time of 1000 ms, in-plane matrix of 64 × 64, field-of-view of 2.3 cm × 2.0 cm, slice thickness of 2 mm, over 4 contiguous slices. All data were collected within 2 hours from the bolus DEX administration.

Data analysis

All the data were analyzed using Matlab (Mathworks, Natick, MA). Optical images, LFP, CBF data, and BOLD fMRI were averaged over multiple runs from identical stimulus frequency conditions. Analyses were performed on each rat separately before group averaging. All graphs including scatter plots, box plots and power law curve fitting were made using Origin 7 (OriginLab Corp., MA).

Flavoprotein autofluorescence imaging map—To determine forepaw area, activation maps were generated from flavoprotein autofluorescence images by calculating the relative increase in fluorescence ($\Delta F/F$). The differential image (ΔF) was obtained by subtracting the average image over 1-s prior to stimulation (F) from the average image over the initial 1-s of stimulation. The maps were smoothed using a Gaussian kernel with width of 5 × 5 pixels and pixels over a threshold of > 67% of the largest increase in fluorescence ($\Delta F/F$) were considered as part of the active area (Fig. 1).

Vessel diameter measurement (Experiments #2.2 and #3.3)—Pial arteries and veins were visually distinguished based on the differences in their color under the microscope with white light illumination (arteries are light red, while *veins* are dark red). The intraluminal vessel diameter was calculated from 570-nm optical images by placing a region-of-interest (ROI) with a four-pixel width perpendicular to the vessel direction. The image within the ROI was linearly interpolated and the intensity along the four-pixel direction was then summed to obtain projected intensity profiles. This yielded the intra-luminal vessel profile and its full-width-at-half-minimum (FWHM) was measured. Assuming the vessel is cylindrical, the actual diameter corresponds to 15.5% over the FWHM value (Vazquez *et al.*, 2010a).

For the study of evoked vessel diameter changes, feeding arteries and draining veins of the active area were chosen. To evaluate whether vessel diameter changed during stimulation, vessel diameters sampled from 5-s prior to stimulation and the 10-s stimulation period were compared using a Kruskal–Wallis test (one-way analysis of variance by ranks). If a significant difference was found in the median ($p < 0.05$), the vessel diameter was considered to significantly change with stimulation. To calculate evoked vessel diameter changes as a function of time (Experiment #3.3), the vessel diameters were normalized by their baseline value (5 s prior to stimulation onset). The maximal diameter change during the 10-s stimulation period was then extracted after low-pass filtering the time course with a cut-off frequency of 2 Hz. To examine the dynamic properties of the changes in vessel diameter, normalized time courses were averaged across all active arteries and veins.

LFP, MUA and CBF data—The evoked LFP data were first fully rectified and summed over the 10-s stimulation period. The summed LFP data were then multiplied by the sampling (0.001 s). For the baseline neural activity data (Experiment #2.1), the mean spike firing rate and LFP power spectral bands were determined for the 5-min recording in each rat. MUA and LFP signals were separated by band-pass filtering between 400 Hz – 1 kHz and 3.3 – 88 Hz, respectively. To determine the mean spike firing rate (spikes/s), a one

standard deviation (SD) threshold was applied for the ISO only and DEX + ISO conditions (the SD from both anesthesia conditions were averaged). A spike was considered present for each 1 ms time point where the MUA intensity exceeded the SD threshold (i.e., 1 spike/ms). The spike firing rate was obtained for each 1-s time bin and the mean spike firing rate for 5 min was calculated. To determine the LFP power over specified spectral bands, the 5-min LFP data were Fourier-transformed. Then, spectrum was divided into delta (1 – <4 Hz), theta (4 – <8 Hz), alpha (8 – <13 Hz), beta (13 – <30 Hz), and gamma (30 – <50 Hz).

The CBF data were low-pass filtered with a 5 Hz cut-off frequency. The filtered CBF data were then normalized by their baseline value (5 s period prior to stimulation onset). The normalized CBF responses were summed over the 10-s stimulation period and multiplied by the sample rate of 0.01 s. To examine the dynamic properties of the changes in CBF, each time course was normalized by its peak intensity and averaged across all animals.

BOLD fMRI—Correlation coefficients were calculated between the voxel-wise time courses and a canonical reference function (which type?). The fMRI data recorded for 8 Hz stimulation were used to determine the ROI for analyzing frequency-dependent studies. The ROI was defined as the 20 voxels with the highest correlation coefficients in the forepaw cortical area. Then, time courses were obtained from the ROI, and percent signal changes were calculated from the baseline, the average value over the 5 s period prior to stimulation onset. Positive BOLD responses were obtained during the 10-s stimulation period, while a post-stimulus undershoot was observed 5 to 25 s after stimulation offset. In each rat, average positive BOLD responses were determined for the five stimulation frequencies and these were normalized by their maximum to reduce inter-animal variation.

Statistical analysis

Nonparametric statistical tests were used to compare medians. Probability values (p) < 0.05 were considered to be statistically significant. All data are expressed as median and interquartile range (IQR), unless otherwise specified.

RESULTS

Blood gas measures of all experiments and their statistical results (Mann-Whitney U-test, Bonferroni corrected) are reported in Table 2. For non-fMRI experiments, DEX administration significantly reduced P_{O2} ($p = 0.0002$,) and S_{O2} level ($p = 0.0054$) and increased Hct ($p = 0.0048$) and Hb ($p = 0.0051$) concentration although they remained within normal physiological ranges (see ISO only vs. DEX50 + ISO for Non-fMRI in Table 2). No significant difference was found in blood gas measurements between DEX + ISO and DEX only conditions. For fMRI experiments, no significant difference was found in the blood gas measurement between ISO only and DEX + ISO conditions. However, P_{CO2} was significantly lower in non-fMRI experiments ($p = 0.0046$, see DEX + ISO (non-fMRI) vs. DEX + ISO (fMRI) in Table 2), possibly due to hypocapnic conditions the lower number of animals used for fMRI studies.

Dexmedetomidine and isoflurane combination for functional studies

Dexmedetomidine only (Experiment #1.1)—In almost all MED-sedated rat fMRI studies recording was performed under MED only (typically 100 μg/kg/h, equivalent to DEX of 50 μg/kg/h). Therefore, somatosensory evoked LFP and CBF responses from forepaw cortical area in five rats were first recorded under DEX only (50 μg/kg/h, IV) (Fig. 2A, left column). While robust, stimulation frequency-dependent CBF responses were observed, consistent with earlier fMRI studies (Zhao *et al.*, 2008; Pawela *et al.*, 2009), periods of epileptic neural discharges followed by electrical silence were also observed,

resulting in abnormally prolonged CBF responses (see open arrow heads above the LFP and CBF traces in Fig. 2A left column). Epileptic responses to 10-s stimulation were observed in runs at 119–177 min after the initial DEX administration in four of the five rats tested (note: the DEX dose rate was modified for the remaining rat prior to the time period where epileptic activity was observed (see Fig. 2B)). These results suggest that evoked responses are prone to become epileptic when DEX is infused at a rate of 50 μg/kg/h for longer than 120 min.

To attempt to avoid this epileptic effect, the DEX dose was increased from 50 to 150μg/kg/h after 120 min from the initial dose in three rats (see two animals' data in Fig. 2). However, epileptic LFP and CBF responses were elicited as soon as stimulation studies were started (see Fig. 2A, right column and 2B) in all three rats tested. Changes in MABP did not correlate with, nor preceded, the initiation of the epileptic discharges, suggesting that a systemic physiological perturbation did not trigger the epileptic-like incident at these dose rates (compare MABP and LFP traces in Fig. 2, A and B). However, supplementing the intravenous DEX administration at 50 μg/kg/h with inspired ISO at 0.1 – 0.5% successfully mitigated the stimulation-evoked epileptic response in 15 of 16 rats over a median recording time of 188 min (IQR = 79.3 min, minimum = 123 min, maximum = 306 min). Only one rat exhibited epileptic responses 171 min after the initial DEX administration under DEX + ISO at 0.5%. Therefore, the rest of the experiments were performed under DEX at 50μg/kg/h (IV) and ISO (0.1–0.5%, typically ~0.3%) to avoid the possible development of epileptic responses.

Dexmedetomidine with nitrous oxide (Experiment #1.2)

Inhalational N_2O is widely used with other anesthetics to enhance analgesic effects in clinical, veterinary and research settings. However, N_2O is an NMDA receptor antagonist (Jevtovic-Todorovic *et al.*, 1998; Mennerick *et al.*, 1998) which is known to reduce hemodynamic responses (Norup Nielsen & Lauritzen, 2001; Gsell *et al.*, 2006). Indeed, inhaled N_2O suppresses somatosensory-evoked hemodynamic responses in combination with ISO at ~1.4% in rats (Masamoto *et al.*, 2007; Kim *et al.*, 2010). Thus, the effect of supplementary inhalational N_2O on LFP and CBF responses was also tested in seven DEX-sedated rats (Fig. 3). As a control, evoked LFP and CBF responses were first recorded under DEX + ISO in oxygen-enriched air (30% O_2 and 70% N_2). ISO was then discontinued and the inspired air was replaced with a mixture of 30% O_2 and 70% N_2O. No significant changes in vascular physiological parameters were found (Table 3). Additionally, N_2O inhalation did not change the baseline CBF (see control vs. test panels in Fig. 3A, left panel in Fig. 3B). However, the evoked LFP responses at 6 and 9 Hz under N_2O were significantly smaller than those in the control condition ($p = 0.0262$ for 6 Hz and $p = 0.0478$ for 9 Hz, $n = 7$ rats, Mann-Whitney U-test). Similarly, the evoked CBF responses at 6, 9 and 12 Hz under N_2O were significantly smaller than those under the control condition ($p = 0.0111$ for 6 Hz, $p = 0.0006$ for 9 Hz, $p = 0.0379$ for 12 Hz, $n = 7$ rats, Mann-Whitney U-test). Upon replacement of the O_2-N_2O breathing mixture with ISO and O_2-enriched air, both LFP and CBF responses were fully recovered (see recovery, right panel in Fig. 3A and Fig. 3B), although the CBF response at 9 Hz in the recovery condition was significantly larger than that under control conditions ($p = 0.0221$, $n = 7$ rats, Mann-Whitney U-test).

Overall, N_2O significantly suppressed CBF responses to a larger extent than LFP responses (middle vs. right panel in Fig. 3B). For instance, the CBF response to 9 Hz stimulation under DEX + N_2O was only 28% (median) of the response under DEX + ISO, while the LFP response was 87% of the control. These results suggest that supplementary ISO (<0.5%) is a more suitable combination to DEX than N_2O.

Dexmedetomidine with isoflurane (Experiment #1.3)—The use of supplementary ISO, a known vasodilator, did not seem to affect the baseline CBF level under DEX anesthesia (e.g., compare Figs. 2 and 3). Similarly, at a level of 0.5%, ISO did not appear to decrease the amplitude of the evoked LFP response; however, the amplitude of the CBF response was slightly smaller that that obtained under DEX-only sedation (e.g., compare Figs. 2 and 3), though still robust. Compared to ISO only, DEX + ISO significantly increased evoked response amplitudes. At a median time of 91.0 min (IQR = 16.0 min) after the initial DEX administration, the LFP and CBF responses to 10-s, 8-Hz forepaw stimulation under DEX + ISO were 1.5 and 3.7 times larger than those under ISO-only, respectively (both LFP and CBF responses became significantly larger, $p = 0.0313$, $n = 6$ rats, Wilcoxon signed rank test). No significant difference in MABP was found between these two conditions ($p = 0.1563$, $n = 6$ rats, Wilcoxon signed rank test). Our data indicate that DEX + ISO enhances evoked hemodynamic responses significantly.

However, this robust CBF response under the DEX- ISO anesthesia was not sustainable over a long experimental time window despite preserved LFP responses (Fig. 4). In general, the CBF response was robust over the initial 120 – 180 min. The baseline CBF level tended to decrease over time, becoming unstable. In addition, the MABP tended to decrease over time, although it remained within a normal physiological range (80 – 120 mmHg). Thus, it was necessary to decrease the supplementary ISO level during the course of experimental recording to maintain MABP and obtain robust evoked CBF responses. When the supplementary ISO level was decreased below 0.1%, evoked responses occasionally became epileptic, and thus the ISO level was always maintained above 0.1% (typically, ~0.3%).

Effects of dexmedetomidine-isoflurane anesthesia on baseline physiology

Different anesthetics modulate spontaneous neuronal activity and baseline CBF differently (Masamoto *et al.*, 2007). Even with the same anesthetics, the baseline activity is modulated dose-dependently and affects evoked responses (Masamoto *et al.*, 2009). Therefore, the effect of DEX on baseline neuronal activity and CBF was examined. Bolus administration of DEX (50 μg/kg, IV) induced bradycardia and a transient increase in MABP followed by a gradual decrease in MABP over time by affecting peripheral nervous system, consistent with earlier reports (Scheinin *et al.*, 1989; Vickery & Maze, 1989; Bari *et al.*, 1993).

Spontaneous neuronal activity (Experiment #2.1)—Under DEX-ISO anesthesia, MUA was more phasic and the LFP waveforms were broadened (Fig. 5A), suggesting more synchronous neuronal activity. The mean spike firing rate significantly increased from a median of 3.5 to 6.9 spikes/s (Fig. 5B) by DEX administration ($p = 0.00049362$, $n = 9$ rats, Mann-Whitney U-test). To quantify the effect of ISO-only and DEX-ISO conditions on LFP activity, LFP power spectra bands were compared (Figure 5C). DEX increased delta band power significantly ($p = 0.0040$, $n = 9$ rats, Mann-Whitney U-test), while it significantly decreased beta and gamma bands power ($p = 0.0040$ for beta and 0.0005 for gamma bands, Mann-Whitney U-test).

Baseline vessel diameter (Experiment #2.2)—To examine whether basal CBV is changed by DEX, pial vessel diameters were measured before and after DEX administration (Fig. 6). Clearly, DEX constricted both arteries (marked as ‘A’ in Fig. 6A) and veins (marked as ‘V’). The constriction reached plateau 30 min after the initial bolus administration (Fig. 6B). This observation was consistent in 15 of the 16 animals studied. The medians of arterial and venous diameters 67.5 min (IQR = 7 min) after initial DEX administration were 77% ($n = 94$) and 74% ($n = 331$) of those under ISO only, respectively (Fig. 6C). No significant difference was found between arterial and venous changes ($p = 0.7546$, Mann-Whitney U-test), suggesting that systemic DEX administration equally

constricts pial arteries and veins. The degree of constriction was related to the vessel diameter, so that larger diameter of vessels constricted by greater amounts (Spearman's rank correlation, rs(94) = −0.4031, p = 0.000064899 for artery; rs(331) = −0.1487, p = 0.0067 for vein).

Baseline cerebral blood flow (Experiment #2.2)—The systemic administration of DEX significantly decreased the baseline CBF in all 15 rats studied as shown in Figure 6D (P = 0.00022289, n = 15 rats, Wilcoxon rank sum test). The median CBF baseline in the DEX + ISO condition was 47% of that in the ISO only condition, suggesting that intracortical vessels may also constrict.

Characterization of neuronal and vascular responses under dexmedetomidine-isoflurane anesthesia

The optimal stimulation frequency varies depending on anesthetic used (Masamoto *et al.*, 2007). Zhao *et al.* (2008) examined that the dependence of the hemodynamic response amplitude on forepaw stimulation frequency in MED-only anesthetized rats and found that the largest BOLD fMRI response was observed at 9 Hz although no significant difference was found when the response was compared to those at 6 – 15 Hz. Here we examined that the impact of supplemental ISO administration on neuro-vascular responses as a function of forepaw stimulation frequency by measuring LFP, CBF and BOLD fMRI.

Local field potential and cerebral blood flow (Experiment #3.1)—To determine the stimulation frequency tuning for LFP and CBF responses, their evoked responses at five different stimulation frequencies were measured from seven rats (Fig. 7A). Responses obtained were normalized by the maximum value within each rat to reduce inter-animal variation (Fig. 7B and 7C). Both LFP and CBF responses differed significantly as a function of stimulation frequencies (Kruskal-wallis test, $\chi^2(4, N = 35) = 26.7897$, p = 0.000021923 for LFP; $\chi^2(4, N = 35) = 26.3893$, p = 0.0000026410 for CBF). A post-hoc analysis (Mann-Whitney U-test, Bonferroni corrected, for a significance level of p = 0.005) revealed that LFP responses at 8 Hz were not significantly different from 10 Hz (p = 0.0087), but these were significantly larger (p = 0.0006) than responses at the other frequencies (Fig. 7B). Similarly, the CBF response at 8 Hz was significantly larger (p = 0.0006, Mann-Whitney U-test, Bonferroni corrected) than responses at all other frequencies (Fig. 7B).

Although the LFP and CBF responses had the same optimal frequency (i.e., 8 – 10 Hz), their tuning curves differed significantly (Friedman test – two-way analysis of variance by ranks – $\chi^2(1, N = 7) = 21.5753$, p = 0.00000034020), indicating a nonlinear relationship between LFP and CBF responses. The relationship observed between the LFP and CBF responses (Fig. 7C) was well described by a power-law function ($CBF = a \cdot LFP^b$, where $a = 1.03 \pm 0.09$ and $b = 3.84 \pm 0.70$, $R^2 = 0.94$). Under DEX-only conditions, CBF was well described by $a \cdot LFP^b$, where $a = 1.00 \pm 0.10$ and $b = 3.23 \pm 0.86$ ($R^2 = 0.90$) (data not shown), suggesting no change in neurovascular coupling by supplemental administration of ISO.

Stimulation frequency-dependent BOLD fMRI (Experiment #3.2)—BOLD responses evoked by forepaw stimulation were measured from the somatosensory forepaw cortical area in four DEX-ISO anesthetized rats for >3 hours. After approximately 2 – 3 hours from the initial DEX administration, baseline signal oscillations became apparent and the evoked responses became unclear in two rats (not shown). Thus, frequency-dependent BOLD data were averaged over the initial 2 hours after DEX bolus injection. Forepaw stimulation induced significant BOLD responses in the contralateral cortical somatosensory area for all frequencies (see Fig. 8A). Time courses of frequency-dependent BOLD responses from all four rats are shown in Fig. 8B. In all four animals, similar frequency-

dependent trends were observed. The commonly observed post-stimulus undershoot was present regardless of stimulation frequency in all four rats. To obtain stimulation frequency tuning, normalized BOLD signals over the 10-s stimulation period average and over the 20-s post-stimulus offset period average were plotted as a function of stimulation frequency (Fig. 8C). On average, the tunings from both the positive response and the post-stimulus undershoot appeared to be similar; the maximum response was observed at ~10Hz. The optimal frequency found in BOLD fMRI studies was consistent with the LDF-based CBF results in this work as well as with an earlier BOLD-fMRI report under MED only (Zhao *et al.*, 2008).

Evoked pial vessel diameter changes (Experiment #3.3)—Arterial vessel dilation is a major component of the vascular response, while venous vessel dilation is minimal during 10 s forepaw stimulation under either isoflurane or α-chloralose anesthesia (Hillman *et al.*, 2007; Kim *et al.*, 2007; Vazquez *et al.*, 2010a; Zong *et al.*, 2012). To examine whether this is the case for DEX-ISO anesthesia, the diameters of pial arterial and venous vessels were measured (Fig. 9). As seen in a representative example (Fig. 9A), vessel diameter increased not only in pial arteries (red), but also in veins (blue) during forepaw stimulation (subfigure c vs. d and time courses in e). The diameter changes of arterial vessels (red time courses in subpanel e) were larger than those of venous vessels (blue time courses). The maximal diameter changes in feeding arteries and draining veins of the active area from all 11 rats are shown in Fig. 9B; significant dilation of vessels were found in all arteries (n = 38; 3 (2.0) vessels/rat (median and IQR)) during stimulation, while significant diameter changes were found in 85% of veins measured (n = 80/94; 7 (3.3) vessels/rat). Median increases in arterial and venous vessel diameters were 32.2% and 5.8%, respectively (Fig. 9B histogram), which were significantly larger than 0 ($p = 0.000000077397$ for artery (n = 38), $p = 0.00000000069148$ for vein (n = 94), Wilcoxon signed rank test). The change in arterial diameter appeared to be greater in smaller arteries, even though this finding is not statistically significant (Spearman's rank correlation coefficient, $rs(38) = -0.2726$, $p = 0.0979$). No relationship was found between the venous diameter and its change during stimulation ($rs(94) = -0.0687$, $p = 0.5104$).

Finally, the dynamic properties of CBF and vascular responses were examined by plotting normalized time courses of CBF along with arterial and venous diameter changes (Fig. 9C). The diameter changes in both arterial and venous vessels occurred as fast as CBF response. The time-to-return-to-baseline was observed first in CBF, then in the arterial diameter, and lastly in venous diameter. No post-stimulus undershoot was observed in CBF, arterial and venous diameter changes.

DISCUSSION

Dexmedetomidine can elicit epileptic evoked responses

We have demonstrated that forelimb stimulation under continuous administration of DEX of 50 μg/kg/h for approximately more than 2 hours elicited epileptic LFP responses with concomitant large increases in CBF (Fig. 2). Incrementing the dose of DEX (150 μg/kg/h) did not prevent the development of the epileptic response. However, the addition of supplementary isoflurane (e.g., ~0.3%) suppressed the generation of the epileptic activity. Seizure activity associated with α_2-adrenergic receptor agonists (Mirski *et al.*, 1994; Miyazaki *et al.*, 1999; Rainger *et al.*, 2009) can be triggered by several factors. First, if oxygen availability is largely decreased due to CBF reduction (as may happen with the administration of DEX), hypoxic injuries could lead seizure (Jensen *et al.*, 1991). However, S_{O2} did not decrease to hypoxic levels under DEX with or without ISO (Table 2), and CBF appeared to be similar under DEX with or without ISO. Thus, hypoxia is probably not the

mechanism causing the epileptic responses. Second, hyper-excitability induced by hyperglycemia (Schwechter *et al.*, 2003) could cause an evoked epileptic response. However, both ISO and DEX can induce hyperglycemia (Nakadate *et al.*, 1980; DiTullio *et al.*, 1984; Morgan & Montague, 1985; Hikasa *et al.*, 1996; Kawano *et al.*, 2008), but the data showed that only DEX elicited epileptic responses. Thus, hyperglycemia is probably not the primary cause of the epileptic response. Finally, perturbation of central adrenergic effects by DEX is most likely involved in seizure expression. Since lesion of the locus coeruleus – the central adrenergic nucleus and the main target of DEX (Guo *et al.*, 1996) –develops seizure (Oishi & Suenaga, 1982), DEX administration may alternate the net pre-synaptic inhibitory and post-synaptic excitatory balance (Samuels & Szabadi, 2008), eliciting evoked epileptic activity.

Dexmedetomidine supplemented with isoflurane prevents evoked epileptic responses

With supplementary ISO administration at levels higher than 0.1%, the evoked epileptic response was successfully suppressed in this study, possibly due to the enhancement of inhibitory action of γ-aminobutyric acid (GABA) by ISO (for review, see Campagna *et al.*, 2003). Since ISO at 0.1 MAC (0.1 – 0.2%) produces hyperalgesia (Zhang *et al.*, 2000), DEX in combination with ISO between 0.3 – 0.5% is recommended for rat forepaw model studies.

Although supplemental ISO administration with DEX effectively suppressed the development of evoked epileptic responses, it did not seem to stably extend the effects of DEX; that, is robust evoked CBF responses were usually obtained up to at most 3 hours under DEX-ISO anesthesia (Fig. 4). This duration matches with the duration of the sedative effect of DEX; the effective hypnotic duration for DEX at 50 μg/kg/h (IP or MED of 100 μg/kg/h, IV) is approximately 3 hours (Doze *et al.*, 1989; Pawela *et al.*, 2009). Maintaining a stable sedative level is important for experimentation as well as obtaining robust responses. Increasing the blood concentration of DEX (Pawela *et al.*, 2009) would enhance the analgesic effect, but would not extend the sedative effect (Pertovaara *et al.*, 1991; Pertovaara *et al.*, 1994; Ansah *et al.*, 2000). The use of higher ISO concentration could also help enhance the analgesic effect rather than the sedative effect. Receptor desensitization (Reid *et al.*, 1994; Hayashi *et al.*, 1995) or the competitive effect between α_1 and α_2-adrenergic receptors due to a high dose of continuous DEX administration can be related to the attenuation of the sedative effect. Although DEX is highly selective to pre-synaptic α_2-adrenergic receptors which inhibits norepinephrine release from pre-synaptic sites, it also exerts the excitatory effect through post-synaptic α_1-adrenergic receptors when it exceeds a certain dosage (Doze *et al.*, 1989; Schwinn *et al.*, 1991), resulting in attenuation of α_2-mediated effects. Thus, the use of relatively low concentrations of DEX (with ISO or other anesthetics) can potentially extent experimental duration. Recently, the combination of DEX of 30 μg/kg/h and ISO of 0.25% was able to maintain stable fMRI responses up to ~4 hours (Lu *et al.*, 2012).

Dexmedetomidine enhances slow wave synchronous neural activity and evoked neural response

The results show that the LFP delta band power increased under DEX-ISO anesthesia while the beta and gamma band power decreased (Fig. 5), which are consistent with previous EEG findings (Farber *et al.*, 1997). Slow, synchronous, large amplitude EEG are observed under anesthesia, while EEG becomes fast, desynchronous and low amplitude in a wakeful state (Bol *et al.*, 1997; Sloan, 1998; Bol *et al.*, 1999). These synchronous and desynchronous switching can be attributed to changes in membrane potential states of neuronal cells. Membrane potential changes between up and down states under anesthesia, while it is persistently in an up-like state in a wakeful state (Constantinople & Bruno, 2011). Thalamic activity does not seem to be important for the persistent up-like state in the wakeful state,

but norepinephrine seems critical (Constantinople & Bruno, 2011). Since DEX directly inhibits norepinephrine release from the locus coeruleus, slow wave fluctuations (i.e., bimodal up and down states) can become more prominent. The increase in the low frequency band power may also enhance resting state functional connectivity under MED or DEX anesthesia (Pawela *et al.*, 2008; Zhao *et al.*, 2008; Pawela *et al.*, 2009; Williams *et al.*, 2010; Kalthoff *et al.*, 2011; Nasrallah *et al.*, 2012).

The results also show that the evoked LFP response under the DEX-ISO anesthesia was significantly larger than that under ISO-only. A reduction in ISO concentration from 1.4% to <0.5% is the likely reason for the enhancement of the LFP response (Banoub *et al.*, 2003). Besides, DEX has a small effect on sensory-induced neural responses (Li *et al.*, 2003). The differential impact of ISO and DEX on neural activity is not limited to evoked potential amplitudes. In the hippocampus, the BOLD response to identical stimuli depends on the previous stimulation history under MED, but not under ISO (Angenstein *et al.*, 2010; Krautwald & Angenstein, 2011). This suggests that ISO and MED interfere differently with hippocampus neural circuits (Angenstein *et al.*, 2010; Krautwald & Angenstein, 2011). These discrepancies can be explained by the fact that DEX does not involve the GABAergic system, but affects the neuromodulator epinephrine, unlike ISO. In other words, the neurovascular response under DEX should be different across brain regions (e.g., see Fig. 5 in Nasrallah *et al.*, 2012) because the sensitivity to DEX varies across brain regions depending on α_2-adrenergic receptor expression (Talley *et al.*, 1996).

Dexmedetomidine-induced vasoconstriction and CBF reduction

We have demonstrated that DEX at 50 μg/kg/h (IV) decreased baseline CBF and constricted both pial arteries and veins with supplemental ISO administration (Fig. 6). CBF reduction and pial vessel constriction induced by DEX have been well-documented for various species. While the cerebral vasoconstriction is mediated by direct agonist binding to α_2-adrenergic receptors on the cerebral vessels (Nakai *et al.*, 1986), the degree of vasoconstriction depends on the dose, the delivery method (topical vs. systemic), and anesthetics used prior to DEX administration (Karlsson *et al.*, 1990; Zornow *et al.*, 1990; Bari *et al.*, 1993; Fale *et al.*, 1994; McPherson *et al.*, 1994; Ishiyama *et al.*, 1995; Asano *et al.*, 1997; Ohata *et al.*, 1999; Iida *et al.*, 2006) as well as arterial carbon dioxide tension (Ganjoo *et al.*, 1998). For instance, reductions of CBF and pial arterial diameter in hypocapnic rats were larger than those in normocapnic rats.

Although the behavior of pial vessels is expected to be generally correlated with parenchymal vessels, their adrenergic innervations differ. Pial vessels are innervated by nerve terminals derived from peripheral superior cervical sympathetic ganglia, while parenchymal vessels (including capillaries) are innervated by nerve terminals derived from central adrenergic neurons within the brain such as locus coeruleus (Hartman *et al.*, 1972; Vaucher & Hamel, 1995; Paspalas & Papadopoulos, 1996; Cohen *et al.*, 1997). In the peripheral vasculature, vasodilation via sympathetic action and vasoconstriction mediated by smooth muscle receptors affected by DEX are known (for review, see Kamibayashi & Maze, 2000). These different innervations, therefore, might explain the findings observed in one rat although it is not clear why the dissociation between pial and parenchymal vessels' diameter changes happened only in this rat (Fig. 6); that is, the dilation of pial vessels with DEX administration despite a decrease in baseline CBF, an indicative of vasoconstriction in parenchyma.

Dexmedetomidine administration yields robust CBF responses and rapid vasodilation

Evoked CBF responses under DEX + ISO were 3.7 times larger compared to ISO-only, and the increase in LFP activity was 1.5 times larger. Large and rapid evoked hemodynamic

responses under DEX-ISO anesthesia (200–300% changes, Fig. 7; ~2% in BOLD, Fig. 8) are the most notable difference to hemodynamic responses obtained under other anesthetics. This may be the result of the relatively high basal vascular tone induced by DEX (Fig. 6). Additionally, the effect of DEX on astrocyte activity may be considered since astrocytes may be a key mediator of neurovascular coupling (Zonta *et al.*, 2003; Takano *et al.*, 2006). Cortical astrocytes can be directly activated by somatosensory stimulation via norepinephrine-dependent locus coeruleus pathway in addition to the general glutamate-dependent thalamocortical pathway (Bekar *et al.*, 2008). However, the locus coeruleus pathway is unlikely involved in the present study because it is activated only for pain stimulation. Thus, the enhancement of hemodynamic response by DEX is not because of the additional pathway's activation. The enhancement of energy metabolism in cortical astrocyte by DEX (Chen *et al.*, 2000) might have an implication for the enhancement of hemodynamic response. Further studies are necessary to understand the impact of the central adrenergic system on neurovascular coupling.

In other anesthetics, sensory-stimulation evokes a rapid vasodilation in pial arteries followed by a delayed and slow increase in venous CBV. This temporal character has been observed in alpha-chloralose-anesthetized rats during 40-s forepaw stimulation (Zong *et al.*, 2012) and in wakeful mice with a 30-s vibrissa stimulation (Drew *et al.*, 2011). Earlier studies performed under ISO-only (Kim *et al.*, 2007) showed that venous vessels did not dilate significantly during 10-s stimulation. However, venous and arterial dilation were significant in response to 10-s forepaw stimulation under DEX + ISO anesthesia, and the venous dilation was observed to be as fast as the arterial dilation, but was slower to return to baseline (Fig. 9). To our knowledge, dilation of pial veins and the increase in venous CBV in response to such a short stimulation duration has not been found in animals anesthetized with isoflurane, alpha-chloralose or urethane (Hillman *et al.*, 2007; Vazquez *et al.*, 2010a; Drew *et al.*, 2011). This discrepancy can be explained by the fact that DEX constricts pial veins as well as pial arteries unlike other anesthetics. In addition, high basal vascular tone may make veins respond as fast as arteries. CBV increases stemming from venous dilations work to reduce the BOLD response, while a slow return to baseline in venous CBV (venous dilation) (Buxton *et al.*, 1998; Mandeville *et al.*, 1998; Mandeville *et al.*, 1999) can account for the BOLD post-stimulus undershoot observed. Therefore, these findings present the opportunity to investigate the mechanism behind the BOLD response shape as a function of physiological parameters such as vascular tone.

CONCLUSION

The advantage of combination with ISO of ~0.3% and DEX of 50 μg/kg/h is that the suppression of epileptiform-like activity without changing desired DEX effects for at least 3 hours. Thus, DEX-ISO anesthesia will be beneficial for relatively short-term recoverable functional experiments since the effects of DEX can be easily reversed using an α_2-adrenergic receptor antagonist, atipamezole. Our results can be useful not only for designing fMRI experiments with animal models under DEX sedation, but also for interpreting fMRI results obtained under this sedative.

Acknowledgments

We thank Ping Wang for his valuable assistance with the experiments. This work was supported by NIH grants R21-EB006571, K01-NS066131, R01-NS044589, and R01-EB003375.

ABBREVIATIONS

BOLD blood oxygenation level dependent

CBF	cerebral blood flow
CBV	cerebral blood volume
DEX	dexmedetomidine
fMRI	functional magnetic resonance imaging
Hct	hematocrit level
Hb	hemoglobin concentration
IP	intraperitoneal
ISO	isoflurane
IV	intravenous
LFP	local field potential
MED	medetomidine
MUA	multiple unit acitivity
O_2	oxygen
N_2O	nitrous oxide
P_{CO2}	arterial partial pressure of carbon dioxide
P_{O2}	arterial partial pressure of oxygen
SC	subcutaneous
S_{O2}	arterial oxygen saturation level

References

Airaksinen AM, Niskanen JP, Chamberlain R, Huttunen JK, Nissinen J, Garwood M, Pitkanen A, Grohn O. Simultaneous fMRI and local field potential measurements during epileptic seizures in medetomidine-sedated rats using raser pulse sequence. Magn Reson Med. 2010; 64:1191–1199. [PubMed: 20725933]

Angenstein F, Krautwald K, Scheich H. The current functional state of local neuronal circuits controls the magnitude of a BOLD response to incoming stimuli. Neuroimage. 2010; 50:1364–1375. [PubMed: 20114080]

Ansah OB, Raekallio M, Vainio O. Correlation between serum concentrations following continuous intravenous infusion of dexmedetomidine or medetomidine in cats and their sedative and analgesic effects. J Vet Pharmacol Ther. 2000; 23:1–8. [PubMed: 10747237]

Asano Y, Koehler RC, Kawaguchi T, McPherson RW. Pial arteriolar constriction to alpha 2-adrenergic agonist dexmedetomidine in the rat. Am J Physiol. 1997; 272:H2547–2556. [PubMed: 9227530]

Banoub M, Tetzlaff JE, Schubert A. Pharmacologic and physiologic influences affecting sensory evoked potentials: implications for perioperative monitoring. Anesthesiology. 2003; 99:716–737. [PubMed: 12960558]

Bari F, Horvath G, Benedek G. Dexmedetomidine-induced decrease in cerebral blood flow is attenuated by verapamil in rats: a laser Doppler study. Can J Anaesth. 1993; 40:748–754. [PubMed: 8104728]

Bekar LK, He W, Nedergaard M. Locus coeruleus alpha-adrenergic-mediated activation of cortical astrocytes in vivo. Cereb Cortex. 2008; 18:2789–2795. [PubMed: 18372288]

Bekker A, Sturaitis MK. Dexmedetomidine for neurological surgery. Neurosurgery. 2005; 57:1–10. discussion 11–10. [PubMed: 15987564]

Berwick J, Martin C, Martindale J, Jones M, Johnston D, Zheng Y, Redgrave P, Mayhew J. Hemodynamic response in the unanesthetized rat: intrinsic optical imaging and spectroscopy of the barrel cortex. J Cereb Blood Flow Metab. 2002; 22:670–679. [PubMed: 12045665]

Bol C, Danhof M, Stanski DR, Mandema JW. Pharmacokinetic-pharmacodynamic characterization of the cardiovascular, hypnotic, EEG and ventilatory responses to dexmedetomidine in the rat. J Pharmacol Exp Ther. 1997; 283:1051–1058. [PubMed: 9399976]

Bol CJ, Vogelaar JP, Mandema JW. Anesthetic profile of dexmedetomidine identified by stimulus-response and continuous measurements in rats. J Pharmacol Exp Ther. 1999; 291:153–160. [PubMed: 10490899]

Buxton RB, Wong EC, Frank LR. Dynamics of blood flow and oxygenation changes during brain activation: the balloon model. Magn Reson Med. 1998; 39:855–864. [PubMed: 9621908]

Campagna JA, Miller KW, Forman SA. Mechanisms of actions of inhaled anesthetics. N Engl J Med. 2003; 348:2110–2124. [PubMed: 12761368]

Chen Y, Zhao Z, Code WE, Hertz L. A correlation between dexmedetomidine-induced biphasic increases in free cytosolic calcium concentration and energy metabolism in astrocytes. Anesth Analg. 2000; 91:353–357. [PubMed: 10910847]

Cohen Z, Molinatti G, Hamel E. Astroglial and vascular interactions of noradrenaline terminals in the rat cerebral cortex. J Cereb Blood Flow Metab. 1997; 17:894–904. [PubMed: 9290587]

Constantinople CM, Bruno RM. Effects and mechanisms of wakefulness on local cortical networks. Neuron. 2011; 69:1061–1068. [PubMed: 21435553]

Correa-Sales C, Rabin BC, Maze M. A hypnotic response to dexmedetomidine, an alpha 2 agonist, is mediated in the locus coeruleus in rats. Anesthesiology. 1992; 76:948–952. [PubMed: 1350889]

DiTullio NW, Cieslinski L, Matthews WD, Storer B. Mechanisms involved in the hyperglycemic response induced by clonidine and other alpha-2 adrenoceptor agonists. J Pharmacol Exp Ther. 1984; 228:168–173. [PubMed: 6141276]

Doze VA, Chen BX, Maze M. Dexmedetomidine produces a hypnotic-anesthetic action in rats via activation of central alpha-2 adrenoceptors. Anesthesiology. 1989; 71:75–79. [PubMed: 2568769]

Drew PJ, Shih AY, Kleinfeld D. Fluctuating and sensory-induced vasodynamics in rodent cortex extend arteriole capacity. Proc Natl Acad Sci U S A. 2011; 108:8473–8478. [PubMed: 21536897]

Fale A, Kirsch JR, McPherson RW. Alpha 2-adrenergic agonist effects on normocapnic and hypercapnic cerebral blood flow in the dog are anesthetic dependent. Anesth Analg. 1994; 79:892–898. [PubMed: 7978406]

Farber NE, Poterack KA, Schmeling WT. Dexmedetomidine and halothane produce similar alterations in electroencephalographic and electromyographic activity in cats. Brain Res. 1997; 774:131–141. [PubMed: 9452201]

Ganjoo P, Farber NE, Hudetz A, Smith JJ, Samso E, Kampine JP, Schmeling WT. In vivo effects of dexmedetomidine on laser-Doppler flow and pial arteriolar diameter. Anesthesiology. 1998; 88:429–439. [PubMed: 9477064]

Gsell W, Burke M, Wiedermann D, Bonvento G, Silva AC, Dauphin F, Buhrle C, Hoehn M, Schwindt W. Differential effects of NMDA and AMPA glutamate receptors on functional magnetic resonance imaging signals and evoked neuronal activity during forepaw stimulation of the rat. J Neurosci. 2006; 26:8409–8416. [PubMed: 16914666]

Guo TZ, Jiang JY, Buttermann AE, Maze M. Dexmedetomidine injection into the locus ceruleus produces antinociception. Anesthesiology. 1996; 84:873–881. [PubMed: 8638842]

Hartman BK, Zide D, Udenfriend S. The use of dopamine -hydroxylase as a marker for the central noradrenergic nervous system in rat brain. Proc Natl Acad Sci U S A. 1972; 69:2722–2726. [PubMed: 4560699]

Hayashi Y, Guo TZ, Maze M. Desensitization to the behavioral effects of alpha 2-adrenergic agonists in rats. Anesthesiology. 1995; 82:954–962. [PubMed: 7717568]

Hikasa Y, Kawanabe H, Takase K, Ogasawara S. Comparisons of sevoflurane, isoflurane, and halothane anesthesia in spontaneously breathing cats. Vet Surg. 1996; 25:234–243. [PubMed: 9012109]

Hillman EM, Devor A, Bouchard MB, Dunn AK, Krauss GW, Skoch J, Bacskai BJ, Dale AM, Boas DA. Depth-resolved optical imaging and microscopy of vascular compartment dynamics during somatosensory stimulation. Neuroimage. 2007; 35:89–104. [PubMed: 17222567]

Iida H, Ohata H, Iida M, Watanabe Y, Dohi S. Isoflurane and sevoflurane induce vasodilation of cerebral vessels via ATP-sensitive K+ channel activation. Anesthesiology. 1998; 89:954–960. [PubMed: 9778013]

Iida H, Iida M, Ohata H, Michino T, Dohi S. Effects of dexmedetomidine on cerebral circulation and systemic hemodynamics after cardiopulmonary resuscitation in dogs. J Anesth. 2006; 20:202–207. [PubMed: 16897240]

Ishiyama T, Dohi S, Iida H, Watanabe Y, Shimonaka H. Mechanisms of dexmedetomidine-induced cerebrovascular effects in canine in vivo experiments. Anesth Analg. 1995; 81:1208–1215. [PubMed: 7486106]

Jensen FE, Applegate CD, Holtzman D, Belin TR, Burchfiel JL. Epileptogenic effect of hypoxia in the immature rodent brain. Ann Neurol. 1991; 29:629–637. [PubMed: 1909851]

Jevtovic-Todorovic V, Todorovic SM, Mennerick S, Powell S, Dikranian K, Benshoff N, Zorumski CF, Olney JW. Nitrous oxide (laughing gas) is an NMDA antagonist, neuroprotectant and neurotoxin. Nat Med. 1998; 4:460–463. [PubMed: 9546794]

Kalso EA, Poyhia R, Rosenberg PH. Spinal antinociception by dexmedetomidine, a highly selective alpha 2-adrenergic agonist. Pharmacol Toxicol. 1991; 68:140–143. [PubMed: 1677190]

Kalthoff D, Seehafer JU, Po C, Wiedermann D, Hoehn M. Functional connectivity in the rat at 11.7T: Impact of physiological noise in resting state fMRI. Neuroimage. 2011; 54:2828–2839. [PubMed: 20974263]

Kamibayashi T, Maze M. Clinical uses of alpha2-adrenergic agonists. Anesthesiology. 2000; 93:1345–1349. [PubMed: 11046225]

Karlsson BR, Forsman M, Roald OK, Heier MS, Steen PA. Effect of dexmedetomidine, a selective and potent alpha 2-agonist, on cerebral blood flow and oxygen consumption during halothane anesthesia in dogs. Anesth Analg. 1990; 71:125–129. [PubMed: 1973880]

Kawano T, Tanaka K, Mawatari K, Oshita S, Takahashi A, Nakaya Y. Hyperglycemia impairs isoflurane-induced adenosine triphosphate-sensitive potassium channel activation in vascular smooth muscle cells. Anesth Analg. 2008; 106:858–864. table of contents. [PubMed: 18292430]

Kim T, Hendrich KS, Masamoto K, Kim SG. Arterial versus total blood volume changes during neural activity-induced cerebral blood flow change: implication for BOLD fMRI. J Cereb Blood Flow Metab. 2007; 27:1235–1247. [PubMed: 17180136]

Kim T, Masamoto K, Fukuda M, Vazquez A, Kim SG. Frequency-dependent neural activity, CBF, and BOLD fMRI to somatosensory stimuli in isoflurane-anesthetized rats. Neuroimage. 2010; 52:224–233. [PubMed: 20350603]

Krautwald K, Angenstein F. Low frequency stimulation of the perforant pathway generates anesthesia-specific variations in neural activity and BOLD responses in the rat dentate gyrus. J Cereb Blood Flow Metab. 201110.1038/jcbfm.2011.1126

Li BH, Lohmann JS, Schuler HG, Cronin AJ. Preservation of the cortical somatosensory-evoked potential during dexmedetomidine infusion in rats. Anesth Analg. 2003; 96:1155–1160. [PubMed: 12651676]

Lu H, Zou Q, Gu H, Raichle ME, Stein EA, Yang Y. Rat brains also have a default mode network. Proc Natl Acad Sci U S A. 2012; 109:3979–3984. [PubMed: 22355129]

MacDonald E, Scheinin M, Scheinin H, Virtanen R. Comparison of the behavioral and neurochemical effects of the two optical enantiomers of medetomidine, a selective alpha-2-adrenoceptor agonist. J Pharmacol Exp Ther. 1991; 259:848–854. [PubMed: 1682487]

Mandeville JB, Marota JJ, Ayata C, Zaharchuk G, Moskowitz MA, Rosen BR, Weisskoff RM. Evidence of a cerebrovascular postarteriole windkessel with delayed compliance. J Cereb Blood Flow Metab. 1999; 19:679–689. [PubMed: 10366199]

Mandeville JB, Marota JJ, Kosofsky BE, Keltner JR, Weissleder R, Rosen BR, Weisskoff RM. Dynamic functional imaging of relative cerebral blood volume during rat forepaw stimulation. Magn Reson Med. 1998; 39:615–624. [PubMed: 9543424]

Martin C, Martindale J, Berwick J, Mayhew J. Investigating neural-hemodynamic coupling and the hemodynamic response function in the awake rat. Neuroimage. 2006; 32:33–48. [PubMed: 16725349]

Masamoto K, Fukuda M, Vazquez A, Kim SG. Dose-dependent effect of isoflurane on neurovascular coupling in rat cerebral cortex. Eur J Neurosci. 2009; 30:242–250. [PubMed: 19659924]

Masamoto K, Kim T, Fukuda M, Wang P, Kim SG. Relationship between Neural, Vascular, and BOLD Signals in Isoflurane-Anesthetized Rat Somatosensory Cortex. Cereb Cortex. 2007; 17:942–950. [PubMed: 16731882]

McPherson RW, Kirsch JR, Traystman RJ. Inhibition of nitric oxide synthase does not affect alpha 2-adrenergic-mediated cerebral vasoconstriction. Anesth Analg. 1994; 78:67–72. [PubMed: 7505532]

Mennerick S, Jevtovic-Todorovic V, Todorovic SM, Shen W, Olney JW, Zorumski CF. Effect of nitrous oxide on excitatory and inhibitory synaptic transmission in hippocampal cultures. J Neurosci. 1998; 18:9716–9726. [PubMed: 9822732]

Mirski MA, Rossell LA, McPherson RW, Traystman RJ. Dexmedetomidine decreases seizure threshold in a rat model of experimental generalized epilepsy. Anesthesiology. 1994; 81:1422–1428. [PubMed: 7992911]

Miyazaki Y, Adachi T, Kurata J, Utsumi J, Shichino T, Segawa H. Dexmedetomidine reduces seizure threshold during enflurane anaesthesia in cats. Br J Anaesth. 1999; 82:935–937. [PubMed: 10562794]

Morgan NG, Montague W. Studies on the mechanism of inhibition of glucose-stimulated insulin secretion by noradrenaline in rat islets of Langerhans. Biochem J. 1985; 226:571–576. [PubMed: 2986600]

Nakadate T, Nakaki T, Muraki T, Kato R. Adrenergic regulation of blood glucose levels: possible involvement of postsynaptic alpha-2 type adrenergic receptors regulating insulin release. J Pharmacol Exp Ther. 1980; 215:226–230. [PubMed: 6109015]

Nakai K, Itakura T, Naka Y, Nakakita K, Kamei I, Imai H, Yokote H, Komai N. The distribution of adrenergic receptors in cerebral blood vessels: an autoradiographic study. Brain Res. 1986; 381:148–152. [PubMed: 3756494]

Nasrallah FA, Tan J, Chuang KH. Pharmacological modulation of functional connectivity: alpha2-adrenergic receptor agonist alters synchrony but not neural activation. Neuroimage. 2012; 60:436–446. [PubMed: 22209807]

Norup Nielsen A, Lauritzen M. Coupling and uncoupling of activity-dependent increases of neuronal activity and blood flow in rat somatosensory cortex. J Physiol. 2001; 533:773–785. [PubMed: 11410634]

Ohata H, Iida H, Dohi S, Watanabe Y. Intravenous dexmedetomidine inhibits cerebrovascular dilation induced by isoflurane and sevoflurane in dogs. Anesth Analg. 1999; 89:370–377. [PubMed: 10439750]

Oishi R, Suenaga N. The role of the locus coeruleus in regulation of seizure susceptibility in rats. Jpn J Pharmacol. 1982; 32:1075–1081. [PubMed: 6186832]

Paspalas CD, Papadopoulos GC. Ultrastructural relationships between noradrenergic nerve fibers and non-neuronal elements in the rat cerebral cortex. Glia. 1996; 17:133–146. [PubMed: 8776580]

Pawela CP, Biswal BB, Cho YR, Kao DS, Li R, Jones SR, Schulte ML, Matloub HS, Hudetz AG, Hyde JS. Resting-state functional connectivity of the rat brain. Magn Reson Med. 2008; 59:1021–1029. [PubMed: 18429028]

Pawela CP, Biswal BB, Hudetz AG, Schulte ML, Li R, Jones SR, Cho YR, Matloub HS, Hyde JS. A protocol for use of medetomidine anesthesia in rats for extended studies using task-induced BOLD contrast and resting-state functional connectivity. Neuroimage. 2009; 46:1137–1147. [PubMed: 19285560]

Pertovaara A, Hamalainen MM, Kauppila T, Mecke E, Carlson S. Dissociation of the alpha 2-adrenergic antinociception from sedation following microinjection of medetomidine into the locus coeruleus in rats. Pain. 1994; 57:207–215. [PubMed: 7916451]

Pertovaara A, Kauppila T, Jyvasjarvi E, Kalso E. Involvement of supraspinal and spinal segmental alpha-2-adrenergic mechanisms in the medetomidine-induced antinociception. Neuroscience. 1991; 44:705–714. [PubMed: 1684411]

Rainger J, Baxter C, Vogelnest L, Dart C. Seizures during medetomindine sedation and local anaesthesia in two dogs undergoing skin biopsy. Aust Vet J. 2009; 87:188–192. [PubMed: 19382926]

Ramos-Cabrer P, Weber R, Wiedermann D, Hoehn M. Continuous noninvasive monitoring of transcutaneous blood gases for a stable and persistent BOLD contrast in fMRI studies in the rat. NMR Biomed. 2005; 18:440–446. [PubMed: 16158460]

Reid K, Hayashi Y, Guo TZ, Correa-Sales C, Nacif-Coelho C, Maze M. Chronic administration of an alpha 2 adrenergic agonist desensitizes rats to the anesthetic effects of dexmedetomidine. Pharmacol Biochem Behav. 1994; 47:171–175. [PubMed: 7906889]

Samuels ER, Szabadi E. Functional neuroanatomy of the noradrenergic locus coeruleus: its roles in the regulation of arousal and autonomic function part II: physiological and pharmacological manipulations and pathological alterations of locus coeruleus activity in humans. Curr Neuropharmacol. 2008; 6:254–285. [PubMed: 19506724]

Savola JM, Virtanen R. Central alpha 2-adrenoceptors are highly stereoselective for dexmedetomidine, the dextro enantiomer of medetomidine. Eur J Pharmacol. 1991; 195:193–199. [PubMed: 1678707]

Savola MK, MacIver MB, Doze VA, Kendig JJ, Maze M. The alpha 2-adrenoceptor agonist dexmedetomidine increases the apparent potency of the volatile anesthetic isoflurane in rats in vivo and in hippocampal slice in vitro. Brain Res. 1991; 548:23–28. [PubMed: 1678296]

Scheinin H, Virtanen R, MacDonald E, Lammintausta R, Scheinin M. Medetomidine--a novel alpha 2-adrenoceptor agonist: a review of its pharmacodynamic effects. Prog Neuropsychopharmacol Biol Psychiatry. 1989; 13:635–651. [PubMed: 2571177]

Schmeling WT, Kampine JP, Roerig DL, Warltier DC. The effects of the stereoisomers of the alpha 2-adrenergic agonist medetomidine on systemic and coronary hemodynamics in conscious dogs. Anesthesiology. 1991; 75:499–511. [PubMed: 1679615]

Schwechter EM, Veliskova J, Velisek L. Correlation between extracellular glucose and seizure susceptibility in adult rats. Ann Neurol. 2003; 53:91–101. [PubMed: 12509852]

Schwinn DA, Correa-Sales C, Page SO, Maze M. Functional effects of activation of alpha-1 adrenoceptors by dexmedetomidine: in vivo and in vitro studies. J Pharmacol Exp Ther. 1991; 259:1147–1152. [PubMed: 1684815]

Seehafer JU, Kalthoff D, Farr TD, Wiedermann D, Hoehn M. No increase of the blood oxygenation level-dependent functional magnetic resonance imaging signal with higher field strength: implications for brain activation studies. J Neurosci. 2010; 30:5234–5241. [PubMed: 20392946]

Segal IS, Vickery RG, Walton JK, Doze VA, Maze M. Dexmedetomidine diminishes halothane anesthetic requirements in rats through a postsynaptic alpha 2 adrenergic receptor. Anesthesiology. 1988; 69:818–823. [PubMed: 2848424]

Sinclair MD. A review of the physiological effects of alpha2-agonists related to the clinical use of medetomidine in small animal practice. Can Vet J. 2003; 44:885–897. [PubMed: 14664351]

Sloan T, Sloan H, Rogers J. Nitrous oxide and isoflurane are synergistic with respect to amplitude and latency effects on sensory evoked potentials. J Clin Monit Comput. 2010; 24:113–123. [PubMed: 20063047]

Sloan TB. Anesthetic effects on electrophysiologic recordings. J Clin Neurophysiol. 1998; 15:217–226. [PubMed: 9681559]

Takano T, Tian GF, Peng W, Lou N, Libionka W, Han X, Nedergaard M. Astrocyte-mediated control of cerebral blood flow. Nat Neurosci. 2006; 9:260–267. [PubMed: 16388306]

Talley EM, Rosin DL, Lee A, Guyenet PG, Lynch KR. Distribution of alpha 2A-adrenergic receptor-like immunoreactivity in the rat central nervous system. J Comp Neurol. 1996; 372:111–134. [PubMed: 8841924]

Van Camp N, Verhoye M, De Zeeuw CI, Van der Linden A. Light stimulus frequency dependence of activity in the rat visual system as studied with high-resolution BOLD fMRI. J Neurophysiol. 2006; 95:3164–3170. [PubMed: 16394078]

Vaucher E, Hamel E. Cholinergic basal forebrain neurons project to cortical microvessels in the rat: electron microscopic study with anterogradely transported Phaseolus vulgaris leucoagglutinin and choline acetyltransferase immunocytochemistry. J Neurosci. 1995; 15:7427–7441. [PubMed: 7472495]

Vazquez AL, Fukuda M, Kim SG. Evolution of the dynamic changes in functional cerebral oxidative metabolism from tissue mitochondria to blood oxygen. J Cereb Blood Flow Metab. 2012; 32:745–758. [PubMed: 22293987]

Vazquez AL, Fukuda M, Tasker ML, Masamoto K, Kim SG. Changes in cerebral arterial, tissue and venous oxygenation with evoked neural stimulation: implications for hemoglobin-based functional neuroimaging. J Cereb Blood Flow Metab. 2010a; 30:428–439. [PubMed: 19844241]

Vazquez AL, Masamoto K, Fukuda M, Kim SG. Cerebral oxygen delivery and consumption during evoked neural activity. Front Neuroenergetics. 2010b; 2:11. [PubMed: 20616881]

Vickery RG, Maze M. Action of the stereoisomers of medetomidine, in halothane-anesthetized dogs. Acta Vet Scand Suppl. 1989; 85:71–76. [PubMed: 2571281]

Weber R, Ramos-Cabrer P, Justicia C, Wiedermann D, Strecker C, Sprenger C, Hoehn M. Early prediction of functional recovery after experimental stroke: functional magnetic resonance imaging, electrophysiology, and behavioral testing in rats. J Neurosci. 2008; 28:1022–1029. [PubMed: 18234880]

Weber R, Ramos-Cabrer P, Wiedermann D, van Camp N, Hoehn M. A fully noninvasive and robust experimental protocol for longitudinal fMRI studies in the rat. Neuroimage. 2006; 29:1303–1310. [PubMed: 16223588]

White PF, Johnston RR, Eger EI 2nd. Determination of anesthetic requirement in rats. Anesthesiology. 1974; 40:52–57. [PubMed: 4810315]

Williams KA, Magnuson M, Majeed W, LaConte SM, Peltier SJ, Hu X, Keilholz SD. Comparison of alpha-chloralose, medetomidine and isoflurane anesthesia for functional connectivity mapping in the rat. Magn Reson Imaging. 2010; 28:995–1003. [PubMed: 20456892]

Zhang Y, Eger EI 2nd, Dutton RC, Sonner JM. Inhaled anesthetics have hyperalgesic effects at 0.1 minimum alveolar anesthetic concentration. Anesth Analg. 2000; 91:462–466. [PubMed: 10910869]

Zhao F, Welsh D, Williams M, Coimbra A, Urban MO, Hargreaves R, Evelhoch J, Williams DS. fMRI of pain processing in the brain: a within-animal comparative study of BOLD vs. CBV and noxious electrical vs. noxious mechanical stimulation in rat. Neuroimage. 2012; 59:1168–1179. [PubMed: 21856430]

Zhao F, Zhao T, Zhou L, Wu Q, Hu X. BOLD study of stimulation-induced neural activity and resting-state connectivity in medetomidine-sedated rat. Neuroimage. 2008; 39:248–260. [PubMed: 17904868]

Zong X, Kim T, Kim SG. Contributions of dynamic venous blood volume versus oxygenation level changes to BOLD fMRI. Neuroimage. 2012; 60:2238–2246. [PubMed: 22401759]

Zonta M, Angulo MC, Gobbo S, Rosengarten B, Hossmann KA, Pozzan T, Carmignoto G. Neuron-to-astrocyte signaling is central to the dynamic control of brain microcirculation. Nat Neurosci. 2003; 6:43–50. [PubMed: 12469126]

Zornow MH, Fleischer JE, Scheller MS, Nakakimura K, Drummond JC. Dexmedetomidine, an alpha 2-adrenergic agonist, decreases cerebral blood flow in the isoflurane-anesthetized dog. Anesth Analg. 1990; 70:624–630. [PubMed: 1971500]

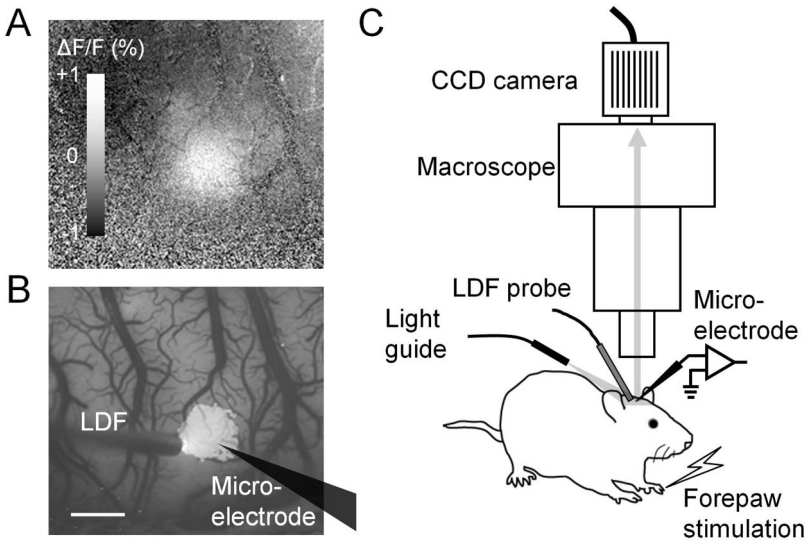

Fig. 1.

Optical imaging of flavoprotein autofluorescence signal and recording setup schematic. **(A)** The cortical forepaw area mapped using flavoprotein autofluorescence is shown from an ISO-anesthetized rat. The white region indicates an increase in autofluorescence evoked by electrical forepaw stimulation. The map was averaged over 0 – 1 s after stimulation onset. The gray scale bar indicates the change in autofluorescence (ΔF) from the pre-stimulation baseline (F). **(B)** Pixels with intensity >67% of its peak intensity (defined as belonging to the hot spot) in the activity map (A) are overlaid on the baseline autofluorescence image. An LDF probe and a microelectrode were placed within or in the vicinity of the hot spot for recording CBF and LFP, respectively. The microelectrode location is drawn on the map. Scale bar, 1 mm. **(C)** Schematic of the recording setup for the forepaw rat model. An LDF probe, microelectrode and light guide were arranged under the microscope. The cortical surface was illuminated with yellow-green light (570 ± 10 nm) and video images were capture every 100 ms with a CCD camera mounted on the microscope.

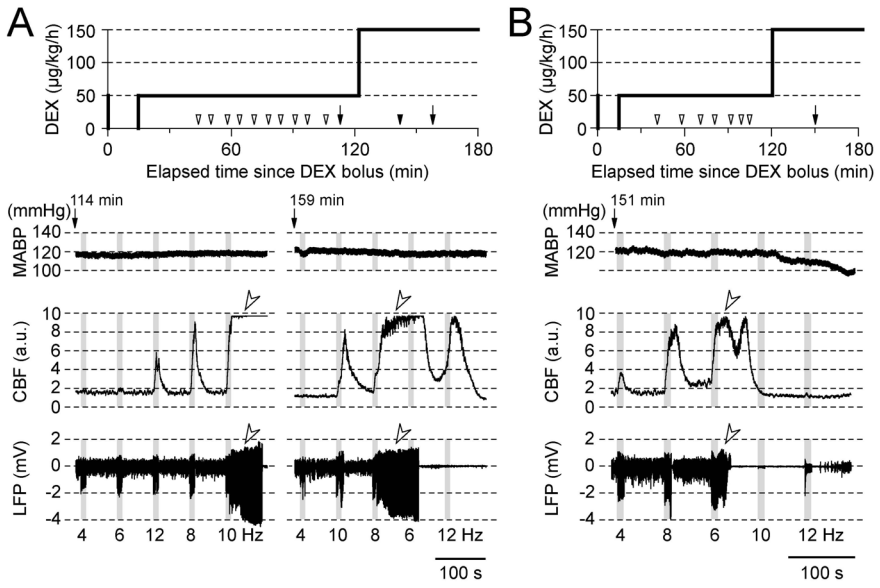

Fig. 2.

CBF and LFP responses in DEX sedative rats without supplemental isoflurane. **(A and B)** Examples obtained from two rats. Evoked responses are prone to induce epileptic activity after approximately 120 min from the initial DEX administration. (1st row) Intravenous infusion of DEX plotted as a function of time from the initial bolus injection of 50 μg/kg (0 min). Open arrowheads on the time scale indicate the beginning of a block of 5 stimulation runs (each consisting of 10-s forepaw stimulation and 70-s ISI). Arrows with filled arrowheads indicate a block containing epileptic responses. Traces of MABP (2nd row), CBF (3rd row) and LFP (4th row) responses are shown from the blocks indicated by the arrows in the 1st raw. The time elapsed from the DEX bolus injection is shown above the MABP trace. Gray vertical bars in each panel indicate 10-s stimulation periods, and the numbers under the LFP traces indicate the stimulation frequency, which were delivered in a pseudo-randomized order. Open arrowheads in CBF and LFP traces point to apparent epileptic responses without any change in MABP.

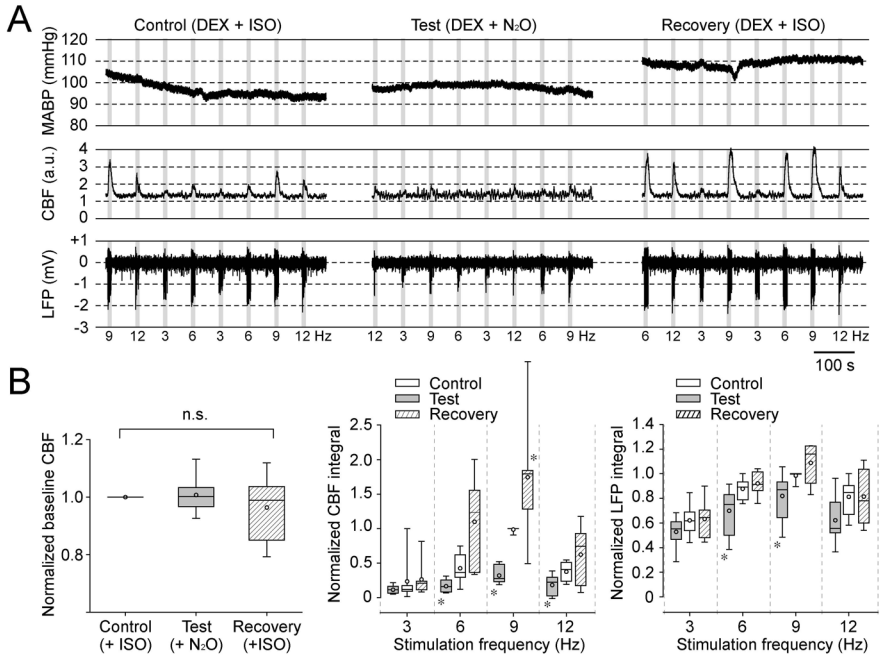

Fig. 3.

Nitrous oxide suppresses evoked CBF responses in DEX-sedative rats. **(A)** An example from one representative rat among 7 rats tested. MABP (1st row), CBF (2nd row) and LFP (3rd row) responses to stimulation at four different frequencies are shown during control (left column), test (middle column) and recovery (right column) conditions. Recording under the control condition started at 104 min after the bolus DEX administration (ISO = 0.27%, O_2 = 29.1%, N_2O = 0.0%); the test condition started at 130 min (ISO = 0.07%, O_2 = 28.9%, N_2O = 69.3%); and the recovery condition started at 150 min (ISO = 0.24%, O_2 = 29.8%, N_2O = 4.06%). Each condition consists of two blocks of two 5 stimulation runs. Gray vertical bars: 10-s stimulation; numbers under LFP traces: stimulation frequency. **(B)** Summary plots from 7 rats (see also Table 3). Box plots for the baseline CBF level (left panel), CBF response amplitude (middle panel), and LFP responses (right panel) for four stimulation frequencies depicted during control (open box), test (gray box) and recovery (shadowed box) conditions. The CBF baseline was normalized to the control condition in each rat. No significant difference (n.s.) was found in the median of the baseline CBF level between control, test and recovery conditions (kruskal-wallis test, χ^2 (2, N = 21) = 1.3015, p = 0.5217). For CBF and LFP responses, the integrals of LFP and CBF responses over the 10-s stimulation period were calculated for each stimulation frequency and normalized to their maximum in each rat. A significant difference was found in the medians of CBF responses between control, test and recovery conditions (Friedman test, χ^2 (2, N = 7) = 33.86, p = 0.0000000443533). Similarly, a significant difference was found in the medians of LFP responses (Friedman test, χ^2 (2, N = 7) = 19.61, p = 0.0000553021). A post-hoc analysis (Mann-Whitney U-test) revealed that CBF responses at 6, 9, and 12Hz, and LFP responses at 9 and 12 Hz in the test condition were significantly smaller than those in the control condition (*, $p < 0.05$). Further, the CBF response at 9 Hz in the recovery condition was significantly larger than control (*, $p < 0.05$).

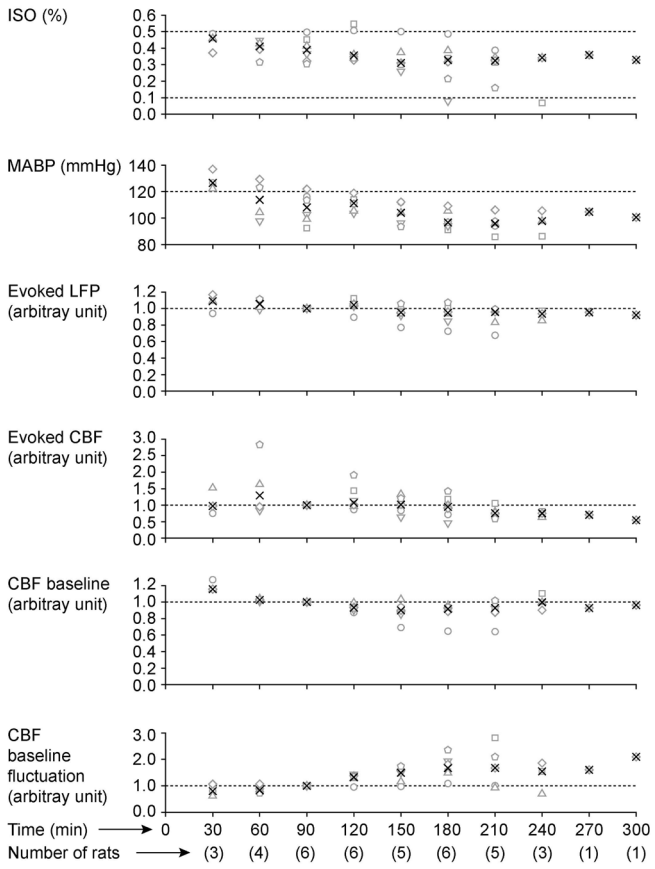

Fig. 4.

Effects of DEX on evoked LFP and CBF responding to 8-Hz forepaw stimulation for an extended recording time. ISO (1st panel), MABP (2nd panel), evoked LFP (3rd panel), evoked CBF (4th panel), CBF baseline (5th panel), and CBF baseline levels (6th panel) are plotted as a function of time. The integral of the evoked CBF and LFP responses for the 10-s stimulation period are shown. Both SD and mean of the CBF baseline for the 5-s pre-stimulation period was obtained, and CBF baseline fluctuation was calculated as SD/mean. The evoked LFP, evoked CBF, CBF baseline and CBF baseline fluctuation were normalized by those at 90 min. At each 30-min time point, data were averaged within ±15 min of the specific time indicated. Different symbols represent different rats, and black cross marks indicate medians.

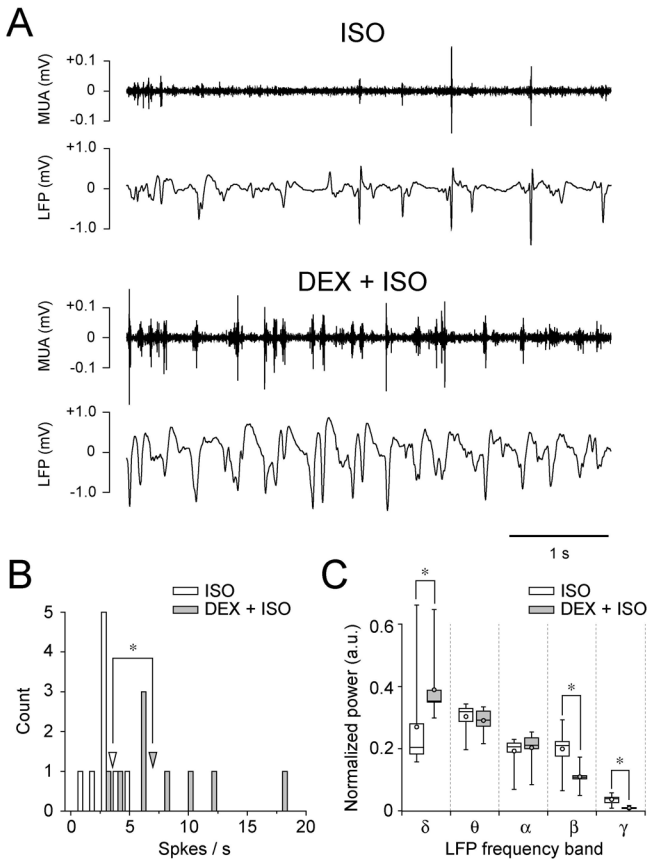

Fig. 5.

Intravenous DEX administration makes MUA phasic and broadens the LFP waveform. **(A)** Spontaneous MUA and LFP recorded for 5 min in one rat are compared to before (upper two traces) and 33 min after DEX (lower two traces) administration. A 5-s segment is shown for better visualization. **(B)** Histogram of spontaneous spike firing rates (open bar, ISO; gray bar, DEX+ISO) with a bin size of 1 s. Open and gray arrowheads indicate the median of spontaneous spike firing rates for ISO (3.5 spike/s) and DEX+ISO (6.9 spike/s) conditions, respectively. These medians are significantly different (*, $p < 0.05$). **(C)** Comparisons of the LFP power bands before and after DEX administration. Results are shown as box plots (open box, ISO; gray box, DEX+ISO). DEX increased the power of the delta band significantly, while it decreased the power in beta and gamma bands significantly (*, $p < 0.05$). In B and C (n = 9 rats), recording was started at a median time of 31.0 min (IQR = 4.3 min) after initial DEX administration. Before and after DEX administration, the median ISO level was 1.3% (IQR = 0.1%) and 0.4% (IQR = 0.1%), respectively; MABP was 84.0 mmHg (IQR = 18.7 mmHg) and 116.1 mmHg (IQR = 23.6 mmHg), respectively.

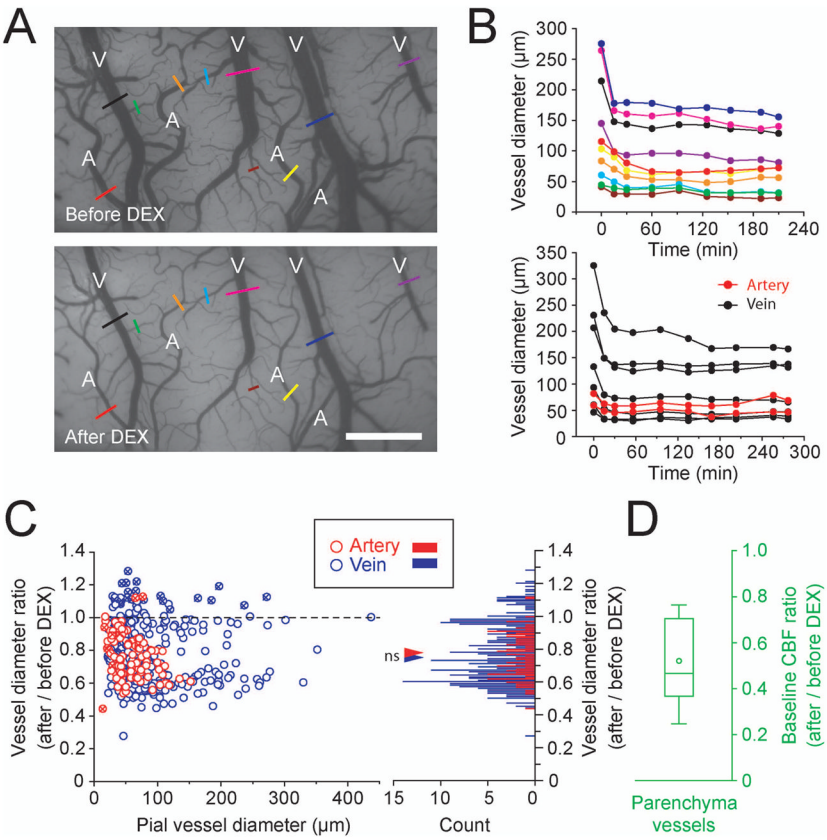

Fig. 6.

Intravenous DEX administration equally constricts pial arteries and veins, and decreases baseline CBF. **(A)** Pial vessel images before and 60 min after bolus DEX administration are shown from one ISO-anesthetized rat. 'A' and 'V' in the image represent arteries and veins, respectively. Quantitative vessel diameters were obtained from the sections indicated by color bars and plotted in the upper panel of B. Scale bar, 1 mm. **(B)** Changes in arterial and venous vessel diameters are shown as a function of time from two rats. Time 0 represents the onset of DEX bolus injection. (Upper panel) Results from the rat shown in A. MABP was gradually decreased from 126.6 to 92.6 mmHg over time, and ISO level was reduced from 0.51 to 0.32% over time. (Lower panel) Results from another rat. Red and black represent arteries and veins, respectively. MABP was gradually decreased from 114.0 to 81.8 mmHg over time, and ISO level was reduced from 0.55 to 0.08% over time. **(C)** Ratios of vessel diameters with and without DEX (94 arteries and 331 veins in 15 rats); 1.0, no diameter change; <1.0, vasoconstriction; >1.0, vasodilation. The effect of DEX on vessel diameter was measured at 67.5 min (IQR = 7 min) after DEX administration. (Left panel) Relationship between vessel diameter changes induced by DEX administration and basal vessel diameters. Red and blue circles indicate artery and vein, respectively. Horizontal broken line indicates no diameter change. Most arteries and veins constrict after DEX administration. Vessel diameters from one rat mostly dilated after DEX bolus administration (circles with ex sign). (Right panel) Histogram of the vessel diameter ratios with a bin size of 0.01. Red and blue triangles indicate the median value in arteries (0.77) and veins (0.74), respectively. No significant difference was found between these medians (Mann-Whitney U-test, p = 0.7546). **(D)** Baseline CBF ratio is shown as a box plot (n = 15 rats). The median basal CBF ratios were 1.3% (IQR = 0.1%) and 0.3% (IQR = 0.1%) before and after DEX

administration with supplemental ISO, respectively, and MABP were 74.6 mmHg (IQR = 22.0 mmHg) and 113.4 mmHg (IQR = 29.9 mmHg), respectively (panels C and D).

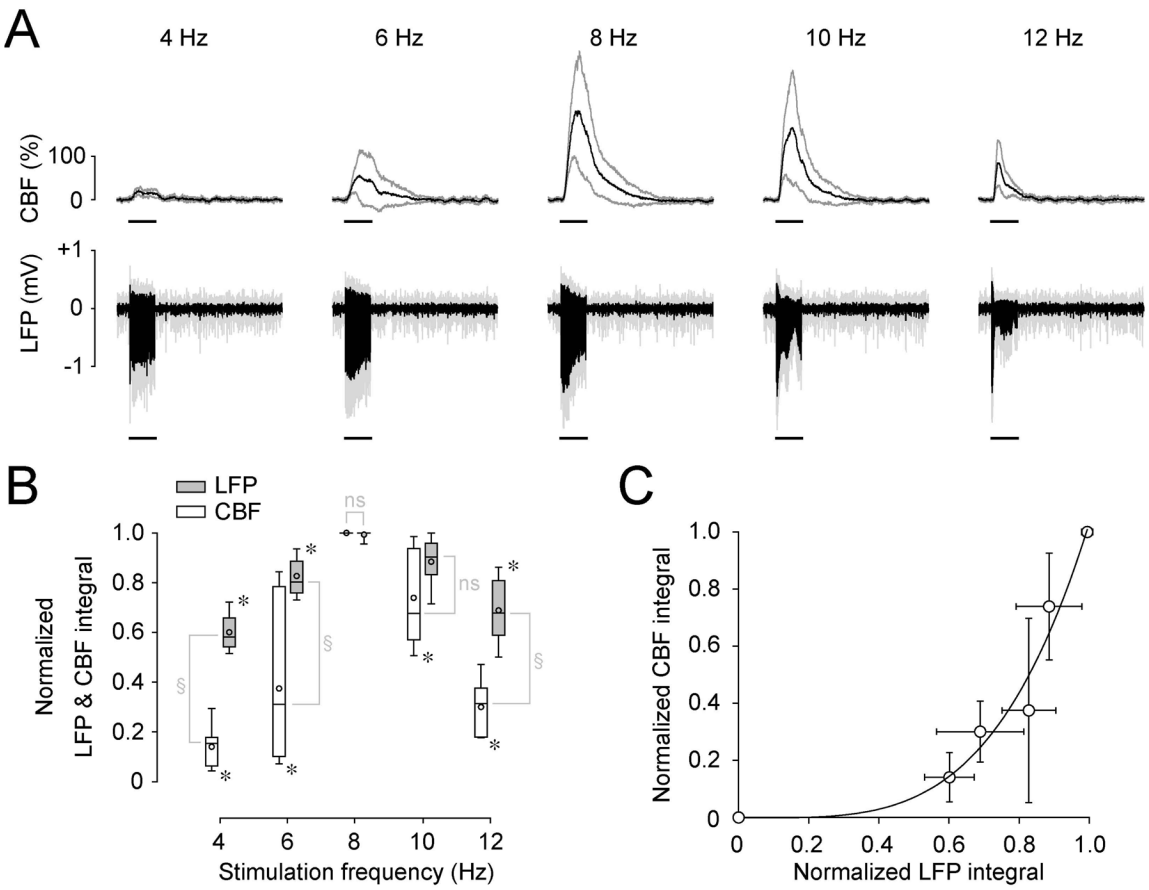

Fig. 7.

CBF and LFP responses under DEX-ISO anesthesia are varied by stimulation frequency. **(A)** The time courses of CBF and LFP responses (mean and standard deviations) from 7 rats are shown for five different stimulation frequencies. A horizontal bar under each trace indicates the 10-s stimulation period. **(B)** The integral of LFP and CBF responses are plotted as a function of stimulation frequency. To reduce inter-animal variations, the integral of these responses were calculated over the 10-s stimulation period for each stimulation frequency and normalized by their maximum in each animal. Results are shown as box plots (open box, CBF; gray box, LFP). The LFP responses at 8 and 10 Hz were not significantly different (ns), but significantly larger than the responses at other frequencies (*, $p < 0.05$). Similarly, the CBF response at 8 Hz was significantly larger than responses at the other frequencies (*, $p < 0.05$). The tuning curves of LFP and CBF responses differ significantly (§, $p < 0.05$). Recording from 7 rats started at a median time of 57.0 min (IQR = 26.3 min) after initial DEX administration and continued for 5 min. Median values for ISO and MABP from 7 rats are 0.4% (IQR = 0.1%) and 119.4 mmHg (IQR = 22.5 mmHg), respectively.. **(C)** Relationship between mean LFP and mean CBF responses (circles in B). A power law represented the data well (solid curve; $CBF = a \cdot LFP^b$), where $a = 1.03 \pm 0.09$ and $b = 3.84 \pm 0.70$ ($R^2 = 0.94$).

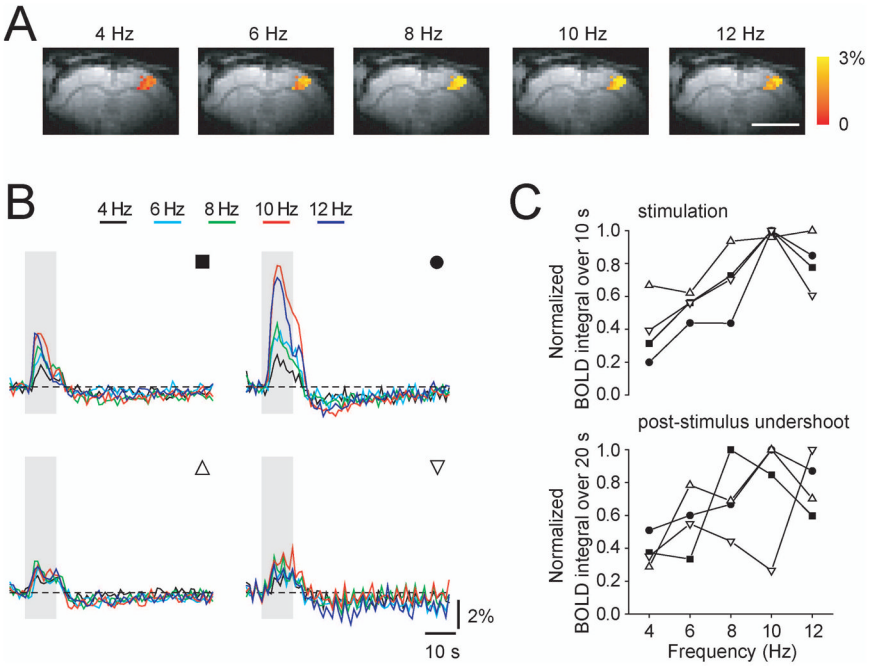

Fig. 8.

Frequency-dependent BOLD fMRI response under DEX-ISO anesthesia. Five different frequencies were used. **(A)** BOLD fMRI maps responding to left forepaw stimulation for five different frequencies in one rat are overlaid on EPI images. Scale, 5 mm. **(B)** BOLD fMRI time courses obtained from active pixels (e.g., color pixles in A). Gray vertical bar indicates a 10-s stimulation period. Upper panels identified by filled symbols were obtained from rats stimulated with 333 μs pulse width and 2.4 mA current, while lower panels identified by open symbols were obtained for 1 ms pulses width and 1.5 mA current. **(C)** Frequency tuning of positive BOLD responses during stimulation (upper panel) and post-stimulus undershoot (lower panel). Different symbols represent different rats (matched with B).

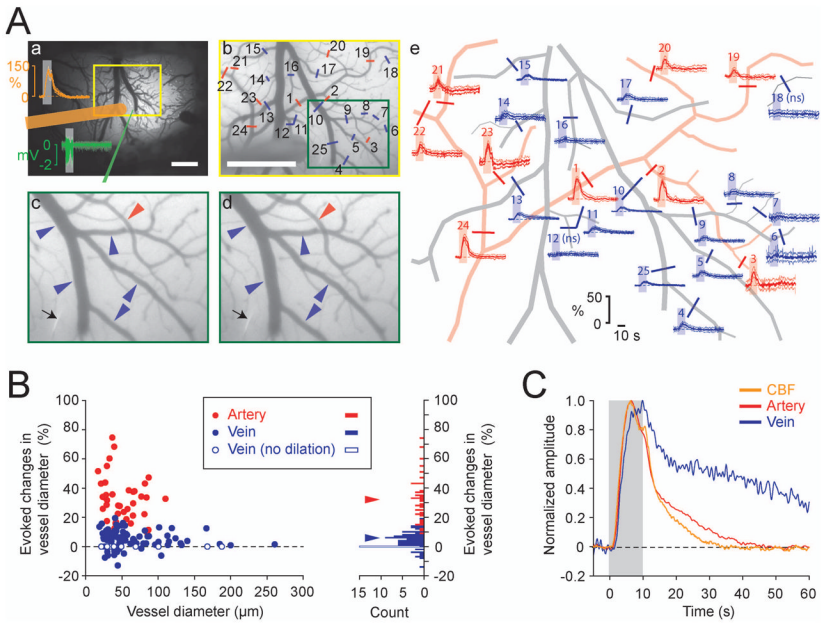

Fig. 9.

Both pial arteries and veins dilate in response to forepaw stimulation under DEX-ISO anesthesia. Data from 11 rats were recorded at a median time of 77.0 min (IQR = 15.5 min) after initial DEX administration. Median values for ISO and MABP from 11 rats were 0.4% (IQR = 0.0%) and 100.9 mmHg (IQR = 0.9 mmHg), respectively. **(A-a)** Forepaw area mapped with flavoprotein autofluorescence signal overlaid on a cortical surface image. Mean (thick trace) and SD (pale trace) of CBF (orange trace) and LFP responses (green traces) during image acquisition for vessel diameter measurement and their measurement sites (orange bar, LDF probe; green line, microelectrode) shown on the image. To record evoked changes in vessel diameters, images were taken from a yellow rectangular region every 100 ms. Scale, 1 mm. **(A-b)** Pre-stimulation image (average of 5 runs) from the yellow rectangular region shown in a. Evoked diameter changes were measured from labeled vessels (red bars on arteries, blue bars on veins) and their time courses are shown in panel e (see, corresponding number). A green rectangular region is expanded in panels c and d for visual inspection of the vessel diameter changes. Scale, 1 mm. **(A-c and d)** Image at the onset of stimulation (c) and image at 10 s (d) from the onset of stimulation (average of 5 runs). Black arrow indicates the microelectrode for LFP recording. Both artery and vein dilate during stimulation (compare vessel diameters pointed by arrow heads (red, artery; blue, vein) between c and d). **(A-e)** Time courses of evoked diameter changes obtained from the vessels labeled on image b (red, artery; blue, vein; Mean and SD, thick and pale traces; horizontal broken line, baseline; gray bar, stimulation period). Major pial vessels seen in panel *b* were traced for better visualization. ns, no significant diameter change. **(B)** Maximal evoked diameter changes during 10-s stimulation for 38 arteries (red) and 80 veins (blue) measured from 11 rats. Median values of the number of arteries and veins measured per rat are 3 (IQR = 2.0) and 7 (IQR = 3.3), respectively. (Left panel) Relationship between evoked vessel diameter changes and basal vessel diameters. Solid circles indicate vessels with significant diameter changes, while open blue circles indicate veins with no diameter change (n = 14). The horizontal broken line indicates no diameter change. No significant relationship is found between basal vessel diameter and diameter changes both in artery and vein. (Right panel) Histogram of the evoked diameter changes with bin size of 1%. Red and blue triangles indicate medians in vessel dilation for arteries (32.2%) and veins (5.8%), respectively. **(C)** Normalized mean time courses of CBF (orange trace), arterial diameter

(red trace) and venous diameter (blue trace) changes (averaged for 11 rats). Gray bar indicates the 10-s forepaw stimulation period. The venous diameter change occurred as fast as the arterial diameter change, but returned to baseline slower than the artery. No post-stimulus undershoot was observed in mean CBF, arterial and venous diameter changes.

Table 1

Summary of experiments

Experiment #	Content	Number of rats	Stimulation	Results
1.1	Evoked LFP and CBF responses under DEX only	5 for 50 μg/kg/h DEX 3 for 150 μg/kg/h DEX	3,4,6,8,9,10, or 12 Hz for 10 s (ISI, 70 s)	Fig. 2
1.2	Comparison between DEX + ISO vs. DEX + N_2O conditions	7	3, 6, 9, and 12 Hz for 10 s (ISI, 70 s), 2 runs for each frequency	Fig. 3
1.3	Effective duration of DEX + ISO for	6	8 Hz for 10 s (ISI, 70 s), typically 2 or 5 runs	Fig. 4
2.1	Baseline MUA and LFP measurements before and after DEX administration	9	Not applicable	Fig. 5
2.2	Baseline CBF and vessel diameter measurements before and after DEX administration	15	Not applicable	Fig. 6
3.1	Frequency-dependent evoked LFP and CBF measurements under DEX + ISO	7	4, 6, 8, 10, and 12 Hz for 10 s (ISI, 70 s), 2 runs for each frequency	Fig. 7
3.2	Frequency-dependent BOLD fMRI measurements under DEX + ISO	4	4, 6, 8, 10, and 12 Hz for 10 s (ISI, 70 s), 10 runs for each frequency	Fig. 8
3.3	Evoked arterial and venous vessel diameter measurements under DEX + ISO	11	8 Hz for 10 s (ISI, 70 s), 10 runs	Fig. 9

Table 2

Blood gas tests

	Non-fMRI				fMRI	
Blood gas Parameters	**ISO only (N = 21)**	**DEX50 + ISO (N = 16)**	**DEX50 only (N = 5)**	**DEX150 only (N = 2)** [a]	**ISO only (N = 4)**	**DEX50 + ISO (N = 4)**
Temperature (°C)	37.4 (0.2)	37.3 (0.3)	37.4 (0.1)	37.3 (0.1)	37.0 (0.2)	37.2 (0.3)
pH	7.511 (0.049)	7.482 (0.049)	7.487 (0.054)	7.470 (0.009)	7.495 (0.037)	7.470 (0.008)
P_{CO2} (mmHg)	36.1 (5.6)	38.2 (4.7)	38.4 (1.6)	37.1 (0.5)	31.8 (4.9) †‡	30.7 (7.1) §
P_{O2} (mmHg)	125.1 (16.0)	108.2 (8.0) *	102.8 (19.1)	108.6 (9.3)	144.3 (15.2) ‡	118.6 (22.5)
S_{O2} (%)	98.6 (1.2)	97.7 (0.9) *	98.3 (1.6)	98.4 (0.3)	98.4 (0.8) *b*	98.2 (0.0) *c*
Hct (%)	37.0 (2.3)	40.0 (4.0) *	38.0 (4.0)	42.0 (2.0)	32.0 (6.0) *b*	34.0 (0.0) *c*
Hb (g/dL)	12.4 (0.6)	13.2 (1.3) *	12.5 (1.2)	13.9 (0.6)	12.4 (0.6) *b*	11.5 (0.0) *c*

All values are presented as median and (interquartile range). ISO, isoflurane (1.3 – 1.4% in ISO only, 0.1 – 0.5% with DEX); DEX50, dexmedetomidine (50 μg/kg/h, IV); DEX150, dexmedetomidine (150 μg/kg/h, IV); N, numbers of rats used; P_{CO2}, arterial partial pressure of carbon dioxide; P_{O2}, arterial partial pressure of oxygen; S_{O2}, arterial oxygen saturation level; Hct, hematocrit level; Hb, hemoglobin concentration. Multiple comparisons were performed for four conditions from non-fMRI experiments. Similarly, multiple comparisons were performed for four conditions from both non-fMRI and fMRI experiments (ISO only and DEX50 + ISO). Thus, the significant p-value of 0.05 is actually 0.0083 after Bonferroni correction.

*P < 0.05 vs. ISO only in non-fMRI group by Mann-Whitney U-test with Bonferroni correction.

†P < 0.05 vs. ISO only in non-fMRI group by Mann-Whitney U-test with Bonferroni correction.

‡P < 0.05 vs. DEX + ISO in non-fMRI group by Mann-Whitney U-test with Bonferroni correction.

§P < 0.05 vs. DEX + ISO in non-fMRI group by Mann-Whitney U-test with Bonferroni correction.

[a]blood gas measures only available for 2 of 3 rats used in this condition.

*b*n = 3.

*c*n = 1.

Table 3

MABP and inspired gaseous concentrations in experiment #1.2

	Control (DEX + ISO)	Test (DEX + N2O)	Recovery (DEX + ISO)
Recording onset time from initial DEX administration (min)	96.0 (10.8)	120.0 (8.3)	141.0 (9.8)
MABP (mmHg)	96.5 (3.3)	98.2 (4.8)	113.8 (11.2)
ISO (%)	0.3 (0.1)	0.07 (0.03)	0.2 (0.1)
O2 (%)	30.8 (2.3)	30.3 (2.4)	30.3 (1.9)
N2O (%)	0.04 (0.00)	67.1 (2.1)	3.7 (1.8)

Values are median and (interquartile range) from 7 rats.

No significant difference is found in MABP medians between control, test and recovery conditions (Kruskal-Wallis test, $\chi^2(2, N = 21) = 4.9647$, $p = 0.0835$). Similarly, no significant difference is found in inspired O_2 medians between control, test and recovery conditions (Kruskal-Wallis test, $\chi^2(2, N = 21) = 0.2301$, $p = 0.8913$).